A

```
p41nox   1   MAGPRYPVSVQGAALVQIKRLQTPAFSVRWSDGSDTFVRRSWDEFRQLKKTLKETFPV
p47phox  1   MGDTFIRHIALLGFEKRFVPSQHYVYMFLVKWQDLSEKVVYRRFTEIYEFHKTLKEMFPI
                 PX
p41nox  58   EAGLLRRSDRVLPKLLDAPLLGRVGRTSRGLARLQLLETYSRRLLATAERVARSPTITGF
p47phox 61   EAGAINPENRIIP---HLPAPKWFDGQRAAENRQGTLTEYCSTLMSLPTKISRCPHLLDF

p41nox  118  FAPQPLDLEPALPPGSRVILPTPEEQPLSRAAGRLSIHS-LEAQSLRCLQPFCTQDTRDR
p47phox 118  FKVRPDDLK--LPTDNQTKKPETYLMPKDGKSTATDITGPIILQTYRAIADYEKTSGS--
                 SH3(N)
p41nox  177  PFQAQAQESLDVLLKHPSGWWLVENEDRQTAWFPAPYLEEAAPGQGREGGPSLGSSGPQP
p47phox 174  EMALSTGDVVEVVEKSESGWWFCQMKAKR-GWIPASFLEPLDSPDETED-PEPNVAGEPY
                 SH3(C)
p41nox  237  CASRAYESSRADELSVPAGARVRVLETSDRGWWLCRYGDRAGLLPAVLLRPEGLGALLSG
p47phox 232  VAIKAYTAVEGDEVSLLEGEAVEVIHKLLDGWWVIRKDDVTGYPPSMYLQKSGQDVSQAQ

p41nox  297  TGFRG-------------------------------------------GDDPAGEARG
p47phox 292  RQIKRGAPPRRSSIRNAHSIHQRSRKRLSQDAYRRNSVRFLQQRRRQARPGPQSPGSPLE
                 autoinhibitory region (AIR)
                 PRR
p41nox  312  FPEPSQATAPPPTVPTRPSPGAIQSRCCTVTRRALERRPRRQGRPRGCVDSVPHPTTEQ
p47phox 352  EERQTQRSKPQPAVPPRPSADLILNRCSESTKRKIASAV
```

B

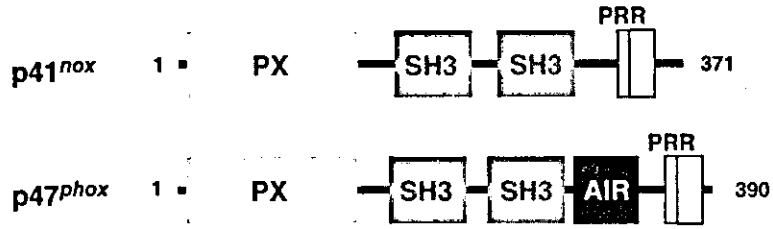

FIG. 1. **Structure of human p41^{nox}, a novel homologue of p47^{phox}.** *A*, deduced amino acid sequence of human p41^{nox} in comparison with human p47^{phox}. Identical amino acid residues are indicated by *asterisks*. *Shaded* are the PX domain, the N-terminal and C-terminal SH3 domains (*SH3(N)* and *SH3(C)*, respectively), the AIR, and the PRR. *Boxed* are the PRR and its C-terminal flanking region. *B*, a schematic representation of the domain arrangement of human p41^{nox} and p47^{phox}.

Hepes-buffered saline (120 mM NaCl, 5 mM KCl, 5 mM glucose, 1 mM $MgCl_2$, 0.5 mM $CaCl_2$, and 17 mM Hepes, pH 7.4). Superoxide production by these cells was determined by SOD-inhibitable chemiluminescence, as described above.

Expression of the p51^{nox} and p41^{nox} Gene in Various Human Tissues—Real time PCR analyses were performed using the ABI PRISM® 7000 Sequence Detection System (Applied Biosystems) according to the manufacturer's instruction. The reaction mixture (25 μl) contained SYBR® Green PCR Master Mix (Applied Biosystems), 0.3 μM each primer, and 2.5 μl of the first strand cDNA from different human tissues (Human MTC™ panels I and II; Clontech) as a template. To quantitate the transcript levels of p41^{nox}, p51^{nox}, Nox1, and glyceraldehyde-3-phosphate dehydrogenase, we used the relative standard curve method as described by Johnson *et al.* (44). The primers used are as follows: 5′-TTCTCTGTGCGCTGGTCAGA-3′ (forward primer) and 5′-TCTTGAGCTGCCTGAATTCGT-3′ (reverse primer) for the p41^{nox} cDNA; 5′-TGGGAGGTGCTACACAATGTG-3′ (forward primer) and 5′-TTGGACATGGCCTCCCTTAG-3′ (reverse primer) for the p51^{nox} cDNA; 5′-TGTGGCCCTCGGACTTTG-3′ (forward primer) and 5′-CCAGACTGGAATATCGGTGACA-3′ (reverse primer) for the Nox1 cDNA; and 5′-GAAATCCCATCACCATCTTCCA-3′ (forward primer) and 5′-CCTTCTCCATGGTGGTGAAGAC-3′ (reverse primer) for the glyceraldehyde-3-phosphate dehydrogenase cDNA.

For Northern blot analysis, human multiple tissue Northern (MTN™) blots (Clontech) were hybridized with a ^{32}P-labeled cDNA fragment, encoding the region that corresponds to amino acids 1–153 of p51^{nox} or amino acids 307–476 of p41^{nox}, under high stringency conditions using ExpressHyb™ (Clontech).

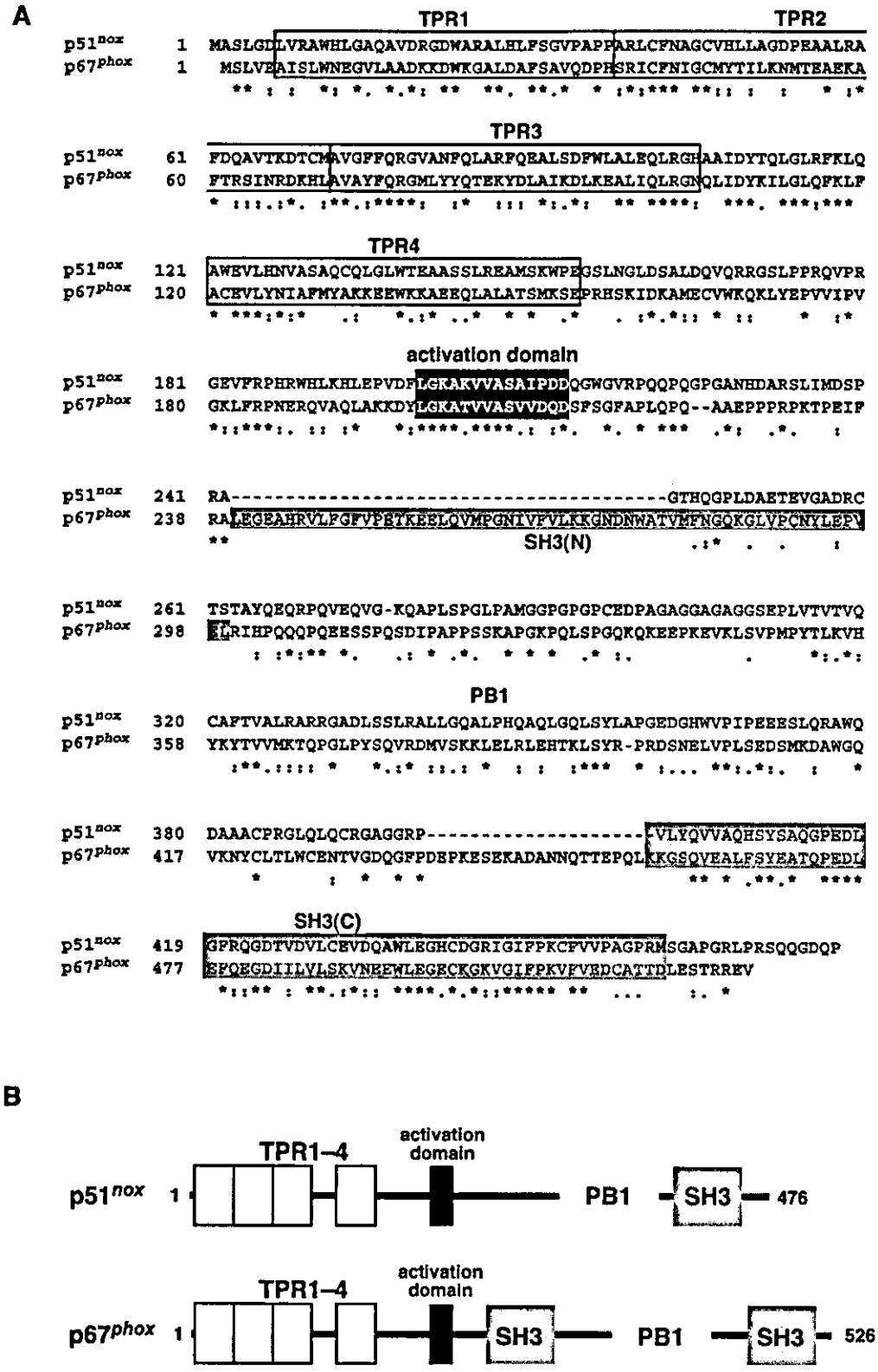

FIG. 2. **Structure of human p51^{nox}, a novel homologue of p67^{phox}.** *A*, deduced amino acid sequence of human p51^{nox} in comparison with human p67^{phox}. Identical amino acid residues are indicated by *asterisks*. *Shaded* are the TPR motifs 1–4, a so-called activation domain, the N-terminal SH3 domain (*SH3(N)*), the PB1 domain, and the C-terminal SH3 domain (*SH3(C)*). *B*, a schematic representation of the domain arrangement of human p51^{nox} and p67^{phox}.

RESULTS

Primary Structure and Domain Architecture of p41^{nox}, a Novel Homologue of p47^{phox}—We have obtained a novel cDNA clone that encodes a protein similar to p47^{phox} (GenBank™ accession number AB097667; for details, see "Experimental Procedures"). Since p47^{phox} is considered to act as an organizer rather than a direct activator of the phagocyte oxidase (see Introduction), the novel gene encoding the p47^{phox} homologue is named NADPH oxidase organizer 1 (NOXO1) after discussion with colleagues working in the field and consultation with

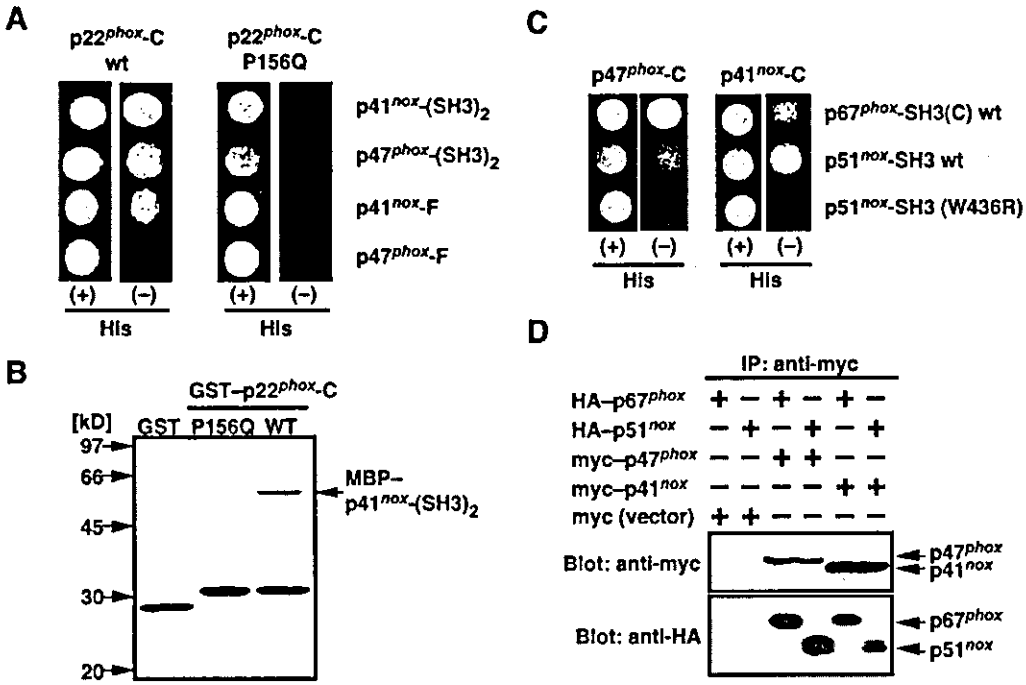

FIG. 3. **Interaction of human p41^{nox} with other oxidase factors.** Interaction of p41^{nox} with p22^{phox} was estimated by the yeast two-hybrid system (*A*) and by an *in vitro* pull-down assay using purified proteins (*B*). *A*, the yeast HF7c cells were cotransformed with a pair of pGBT9 encoding the wild-type p22^{phox}-C (amino acids 132–195) or a p22^{phox}-C carrying the P156Q substitution and pGADGH encoding the isolated tandem SH3 domains or full-length protein of p41^{nox} and p47^{phox}: p41^{nox}-(SH3)$_2$, p47^{phox}-(SH3)$_2$, p41^{nox}-F, or p47^{phox}-F. Following the selection for Trp$^+$ and Leu$^+$ phenotype, its histidine-dependent (*right*) and -independent (*left*) growth was tested as described under "Experimental Procedures." *B*, GST alone, GST-p22^{phox}-C, or GST-p22^{phox}-C(P156Q) was incubated with MBP-p41^{nox}-(SH3)$_2$ and pulled down with glutathione-Sepharose. The precipitated proteins were subjected to SDS-PAGE, followed by staining with Coomassie Brilliant Blue. Positions for marker proteins are indicated in kDa. Interaction of p41^{nox} or p47^{phox} with p51^{nox} or p67^{phox} was estimated by the yeast two-hybrid system (*C*) and by an immunoprecipitation assay using cells expressing the proteins (*D*). *C*, the yeast HF7c cells were cotransformed with a pair of pGBT9 encoding the C terminus of p41^{nox} (*p41^{nox}-C*) or p47^{phox} (*p47^{phox}-C*) and pGADGH encoding p51^{nox}-SH3 or p67^{phox}-SH3(C). Following the selection for Trp$^+$ and Leu$^+$ phenotype, its histidine-dependent (*right*) and -independent (*left*) growth was tested. *D*, COS-7 cells were transfected with a pair of the expression constructs as indicated *above* each *lane*; the constructs were pEF-BOS-Myc-p41^{nox}, pEF-BOS-Myc-p47^{phox}, pEF-BOS-HA-p51^{nox}, and pEF-BOS-HA-p67^{phox}. Lysates of the transfected cells were analyzed by immunoprecipitation (*IP*) with the anti-Myc monoclonal antibody, followed by immunoblot (*Blot*) with the anti-Myc (*upper panels*) or anti-HA (*lower panels*) polyclonal antibodies. For details, see "Experimental Procedures." These experiments have been repeated more than three times with similar results.

Dr. Ruth Lovering (the Human Genome Organization Nomenclature Committee). The NOXO1 cDNA contains an open reading frame of 1,113 nucleotides with the first methionine codon surrounded by a sequence similar to the Kozak consensus (ACAGCCATGG) and an in-frame preceding termination codon. The encoded protein comprises 371 amino acids with a calculated molecular mass of about 41 kDa (Fig. 1), and thus the novel protein was designated as p41^{nox}. When the protein was expressed in COS-7 cells, an apparent molecular mass was estimated at 43–44 kDa by SDS-PAGE analysis (data not shown). Searching the sequence data base revealed that a human genomic contig (GenBank^{TM} accession number NT-010552) that is located on chromosome 16p13 contains an entire region of the p41^{nox} cDNA. The p41^{nox} protein described here is encoded by at least eight exons with exon-intron boundaries, covering a minimum of about 3 kb.

Although the overall amino acid sequence of human p41^{nox} shows only about 23% identity with human p47^{phox} (Fig. 1*A*), the domain arrangements of both proteins are basically conserved; p41^{nox} contains the N-terminal PX domain (45, 46), the two SH3 domains tandemly arranged in the middle, and the C-terminal PRR (Fig. 1*B*). In addition to the PRR of p41^{nox}, its C-terminally flanking region is also similar to that of p47^{phox}, which plays an important role in binding to p67^{phox} together with the PRR (19). On the other hand, p41^{nox} lacks a region that is expected to mask its SH3 domains; the corresponding region of p47^{phox} (amino acids 286–340), the AIR, intramolecularly binds to the SH3 domains, and thereby prevents the domains from binding to the target p22^{phox} (22). The stretch Pro^{299}-Pro^{300}-Arg^{301}-Arg^{303} in the AIR of p47^{phox} directly interacts with the N-terminal SH3 domain (22), and phosphorylation of this region, particularly at Ser-303, Ser-304, and Ser-328, culminates in induction of a conformational change, which renders the SH3 domains in a state accessible to p22^{phox} (22, 26). These amino acids are all missing in p41^{nox}, suggesting that accessibility of the SH3 domains of p41^{nox} is not regulated, and thus the novel protein may act as a constitutively active organizer of the oxidase accordingly.

Primary Structure and Domain Architecture of p51^{nox}, a Novel Homologue of p67^{phox}—We have also cloned a novel human cDNA encoding a protein homologous to p67^{phox} (GenBank^{TM} accession number AB095031; for details, see "Experimental Procedures"). After discussion with colleagues working in the field and Dr. Lovering, the gene has been termed NADPH oxidase activator 1 (NOXA1), because p67^{phox} is likely to function as a direct activator of the phagocyte NADPH oxidase (see Introduction). The cDNA clone contains an open reading frame of 1,428 nucleotides with the first methionine codon, which is surrounded by a sequence that completely agrees with the Kozak consensus (GCCGCCATGG). The predicted protein product of the NOXA1 gene consists of 476 amino acids (Fig. 2*A*). Because of a calculated molecular mass of about 51 kDa, this protein is tentatively designated as p51^{nox}; a slightly higher molecular mass (53–54 kDa) was estimated by SDS-PAGE when expressed in COS-7 cells (data not shown).

Although the overall amino acid sequence of human p51^{nox}

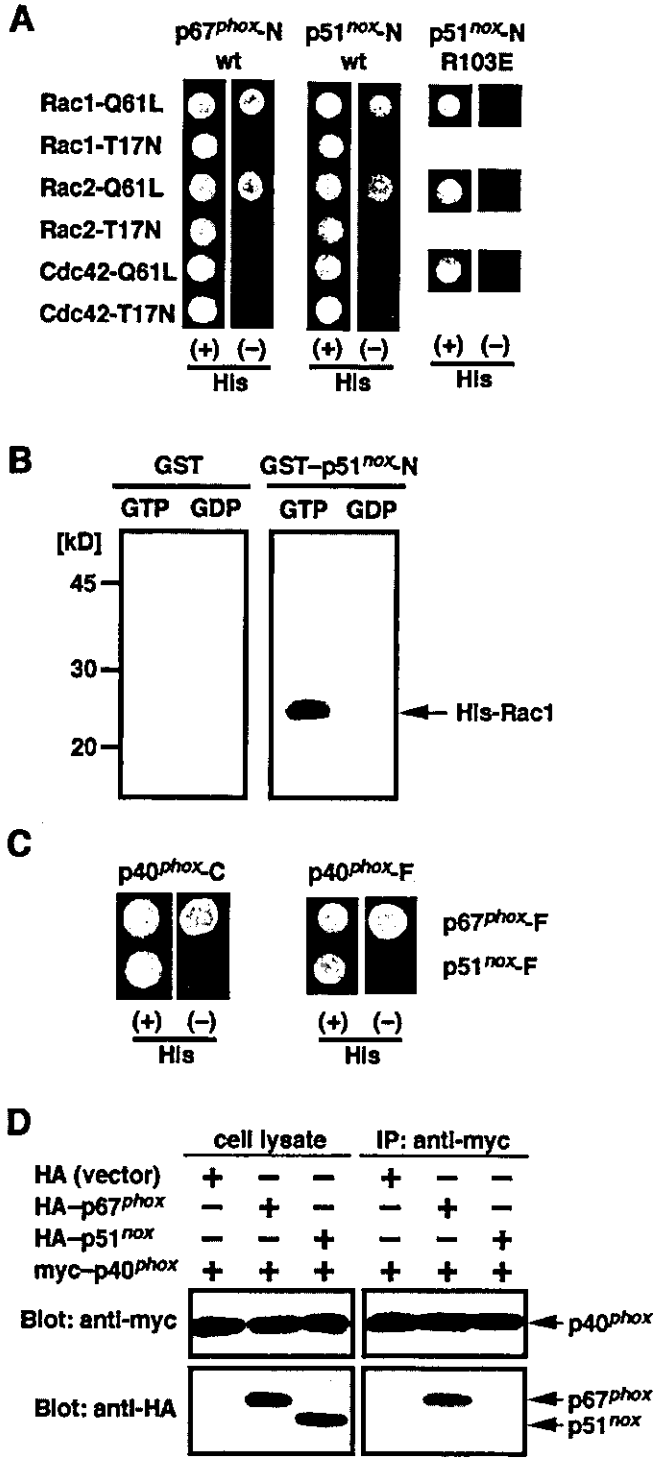

FIG. 4. **Interaction of human p51^{nox} with other oxidase factors.** Interaction of p51^{nox} with Rac (*A* and *B*) or p40^{phox} (*C* and *D*) was estimated by the yeast two-hybrid system (*A*) and by an *in vitro* pull-down assay using purified proteins (*B*). *A*, the yeast HF7c cells were cotransformed with recombinant plasmids pGBT9 encoding Rac1, Rac2, or Cdc42 carrying a mutation and pGADGH encoding the N terminus of the wild-type or a mutant p51^{nox} or p67^{phox}: Q61L (a constitutively active form of the GTPases) and T17N (a dominant negative form of the GTPases). Following the selection for Trp$^+$ and Leu$^+$ phenotype, its histidine-dependent (*right*) and independent (*left*) growth was tested as described under "Experimental Procedures." *B*, GST alone or GST-p51^{nox}-N (amino acids 1–224) was incubated with His-Rac1 (Q61L) containing GTPγS or wild-type Rac1 containing GDP and pulled down with glutathione-Sepharose. The precipitated proteins were subjected to SDS-PAGE, followed by immunoblot analysis with an anti-His antibody. Positions for marker proteins are indicated in kDa. Interaction of p51^{nox} with p40^{phox} was estimated by the yeast two-hybrid system (*C*) and by an immunoprecipitation assay using cells expressing the proteins (*D*). *C*, the yeast HF7c cells were cotransformed with a pair of pGBT9 encoding the full length of p51^{nox} (*p51^{nox}-F*) or p67^{phox} (*p67^{phox}-F*) and pGADGH encoding the full length (amino acids 1–339) or the C terminus (residues 234–339) of p40^{phox} (*p40^{phox}-F* and *p40^{phox}-C*, respectively). Following the selection for Trp$^+$ and Leu$^+$ phenotype, its histidine-dependent (*right*) and -independent (*left*) growth was tested. *D*, COS-7 cells were cotransfected with either pEF-BOS-HA-p51^{nox} or pEF-BOS-HA-p67^{phox} and pEF-BOS-Myc-p40^{phox}, as indicated *above* each *lane*. Lysates of the transfected cells were analyzed by immunoprecipitation (*IP*) with the anti-Myc monoclonal antibody, followed by immunoblot (*Blot*) with the anti-Myc (*upper panels*) or anti-HA (*lower panels*) polyclonal antibodies. Proteins in cell lysates were also analyzed directly by immunoblot. For details, see "Experimental Procedures." These experiments have been repeated more than three times with similar results.

exhibits only about 28% identity with human p67^{phox}, the domain architectures of both proteins are very similar, except that the N-terminal SH3 domain is absent in p51^{nox} (Fig. 2, *A* and *B*). The most conserved region is the C-terminal SH3 domain, with 52% identity, a domain of p67^{phox} known to directly bind to the C-terminal PRR of p47^{phox} (17–19). It is also known that p67^{phox} interacts with p40^{phox} via the Phox and Bem 1 (PB1) domain between the SH3 domains (47). There also exists the PB1-like region in p51^{nox}, but without the conserved lysine, corresponding to Lys-355 of p67^{phox}, that plays an essential role in the interaction with p40^{phox} (40, 47).

The small GTPase Rac directly binds to the N-terminal region of p67^{phox} containing ~200 amino acid residues, an interaction that is essential for activation of the phagocyte NADPH oxidase (28). There exist four TPR motifs in the Rac-binding domain (28, 29), and Arg-102 on the third motif plays a critical role (28); the R102E substitution results in a loss of both the interaction with Rac and the oxidase activation (28). The N-terminal region of p51^{nox} is well conserved, with 39% amino acid identity to that of p67^{phox}; it contains four TPR motifs and keeps the corresponding arginine residue (Arg-103) in the third TPR, suggesting that p51^{nox} may interact with Rac. In addition, an about 10-amino acid stretch, C-terminal to the Rac-binding domain, is highly conserved between p51^{nox} and p67^{phox}. The stretch of p67^{phox}, a so-called activation domain, is required for the phagocyte oxidase activation (48, 49); deletion of the stretch or the V204A substitution leads to an impaired activation of the oxidase (48–50). Thus, p51^{nox} is expected to function as an activator of the phagocyte oxidase gp91^{phox}/Nox2.

p41^{nox} Interacts with p22^{phox} and p67^{phox}—As an initial step to investigate the function of p41^{nox}, we tested the ability of p41^{nox} to bind to other oxidase factors. It is established that p47^{phox} binds via the SH3 domains to the C-terminal tail of p22^{phox}, which plays an essential role in activation of the phagocyte NADPH oxidase. Similarly, the SH3 domains of p41^{nox} bound to the C terminus of p22^{phox}, as estimated in the yeast two-hybrid system (Fig. 3*A*) and by an *in vitro* binding assay using purified proteins (Fig. 3*B*). However, the domains could not interact with a p22^{phox} carrying the P156Q substitution, a mutation that occurs in a patient with chronic granulomatous disease (51, 52). Full-length p47^{phox} (p47^{phox}-F) was incapable of binding to p22^{phox}, since the SH3 domains of p47^{phox} are normally masked via an intramolecular interaction with the AIR (Fig. 3, *A* and *B*; see Refs. 20 and 22). Interestingly, full-length p41^{nox} (p41^{nox}-F) interacted with p22^{phox} (Fig. 3*A*), which appears to be in agreement with the fact that the AIR is absent in p41^{nox} (Fig. 1).

It is also known that p47^{phox} associates with p67^{phox} via the C-terminal region containing the PRR (17–19). As shown in Fig. 3 (*C* and *D*), p41^{nox} was capable of interacting with p67^{phox} as well. The findings suggest the possibility that p41^{nox} may

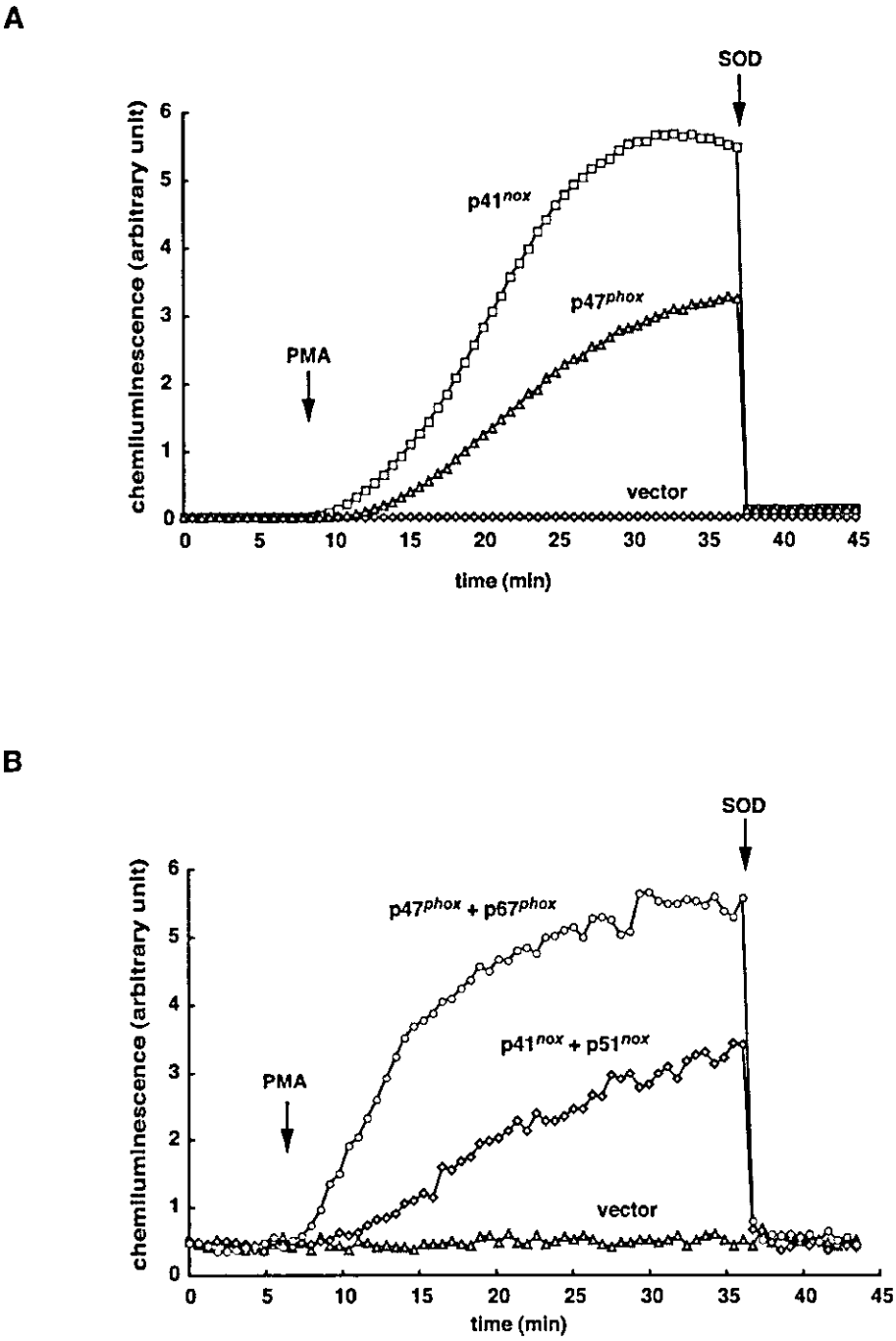

FIG. 5. **Effects of p41^{nox} and p51^{nox} on activation of the phagocyte NADPH oxidase in K562 cells.** *A*, the K562-gp91^{phox}/p67^{phox} cells were transfected with the mammalian expression vector pEF-BOS encoding cDNA for either p41^{nox} or p47^{phox} or pEF-BOS alone. The transfected cells (1×10^5 cells) were stimulated with PMA (200 ng/ml), and chemiluminescence change was continuously monitored with an enhanced luminol-based substrate, DIOGENES. SOD (50 μg/ml) was added where indicated. *B*, the K562-gp91^{phox} cells were transfected with a pair of pEF-BOS-p41^{nox} and pEF-BOS-p51^{nox} or a pair of pEF-BOS-p47^{phox} and pEF-BOS-p67^{phox}. The doubly transfected cells (1×10^5 cells) were stimulated with PMA (200 ng/ml). Chemiluminescence change was continuously monitored with DIOGENES, and SOD (50 μg/ml) was added where indicated. For details, see "Experimental Procedures." These experiments have been repeated more than three times with similar results.

activate the phagocyte oxidase instead of p47^{phox} by interacting with the oxidase factors.

p51^{nox} Interacts with Rac but Fails to Interact with p40^{phox}—In the yeast two-hybrid system, p51^{nox} interacted with Rac1 (Q61L), a constitutively active form, but not with a dominant negative form of Rac (T17N), as p67^{phox} did (Fig. 4*A*). The same interaction was observed when Rac2, but not Cdc42, was used instead of Rac1 (Fig. 4*A*). In addition, p51^{nox} bound to GTP-bound Rac1 in an *in vitro* binding assay using purified proteins, whereas it failed to interact with GDP-bound Rac1 (Fig. 4*B*). Thus, p51^{nox} appears to directly bind to GTP-bound Rac. The substitution of Glu for the conserved arginine Arg-103 in p51^{nox} led to a complete loss of the interaction with Rac (Fig. 4*A*). Thus, p51^{nox} probably recognizes Rac in a similar manner as does p67^{phox}, suggesting that the novel homologue also acts as an oxidase activator.

Furthermore, p51^{nox} was also capable of binding to p47^{phox} and p41^{nox} (Fig. 3*D*). The binding is considered to be mediated via the SH3 domain; the substitution of Arg for Trp-436, the invariant residue among SH3 domains, resulted in a loss of the interaction (Fig. 3*C*). Since p51^{nox} retains the PB1 domain, albeit with a weak similarity (Fig. 2), it seemed possible that p51^{nox} also can bind to p40^{phox}. However, we could not detect interaction between p51^{nox} and p40^{phox} in the yeast two-hybrid system (Fig. 4*C*) or in an immunoprecipitation assay using cells expressing both proteins (Fig. 4*D*), whereas p67^{phox} fully bound to p40^{phox} under the same conditions. These findings appear to be consistent with the fact that the PB1-like region of p51^{nox} lacks the conserved lysine residue corresponding to Lys-355 of p67^{phox} (Fig. 2).

p41^{nox} and p51^{nox} Are Capable of Supporting Activation of the Phagocyte NADPH Oxidase in K562 Cells—To explore the function of p41^{nox}, we transfected the K562-gp91^{phox}/p67^{phox} cells with the mammalian expression vector pEF-BOS encod-

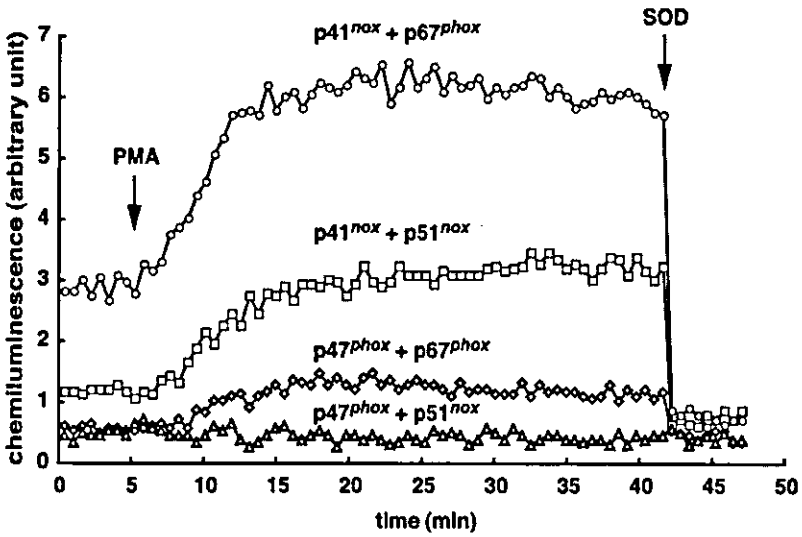

FIG. 6. **Effects of p41^{nox} and p51^{nox} on activation of gp91^{phox} in COS-7 cells.** COS-7 cells were transfected simultaneously with pcDNA3.0-gp91^{phox} and the following pair of pEF-BOS vectors encoding the oxidase organizer and activator homologues: p41^{nox} and p51^{nox}; p41^{nox} and p67^{phox}; p47^{phox} and p51^{nox}; or p47^{phox} and p67^{phox}. The transfected cells (1×10^5 cells) were preincubated for 5 min at 37 °C and then stimulated with PMA (200 ng/ml). Chemiluminescence change was continuously monitored with DIOGENES, and SOD (50 μg/ml) was added where indicated. For details, see "Experimental Procedures." The experiments have been repeated more than three times with similar results.

ing cDNA for p41^{nox} or p47^{phox}. The K562-gp91^{phox}/p67^{phox} cells stably express functional cytochrome b_{558} comprising the two subunits gp91^{phox} and p22^{phox} as well as p67^{phox}, but they do not contain p47^{phox} (22). As shown in Fig. 5*A*, the p41^{nox}-expressing cells fully produced superoxide in response to PMA, a potent stimulant of the phagocyte NADPH oxidase *in vivo*, indicating that p41^{nox} is a functional homologue of p47^{phox}. The activity of p41^{nox} appeared to be higher than that of p47^{phox} (Fig. 5*A*); the difference is not due to their expression level, since immunoblot analysis revealed that essentially the same amounts of these proteins were expressed in the reconstitution system (data not shown). The cooperation of p41^{nox} with p67^{phox} in the oxidase activation agrees with the present finding that p41^{nox}, as well as p47^{phox}, binds to p67^{phox} (Fig. 3, *C* and *D*).

Since p41^{nox} can interact not only with p67^{phox} but also with p51^{nox} (Fig. 3, *C* and *D*), it seems likely that p41^{nox} also functions together with p51^{nox}. To test this possibility, we expressed both p41^{nox} and p51^{nox} in K562-gp91^{phox} cells that express functional cytochrome b_{558} but lack p47^{phox} and p67^{phox} (28). In response to PMA, the K562-gp91^{phox} cells cotransfected with p41^{nox} and p51^{nox} produced superoxide at a level comparable with the cells transfected with p47^{phox} and p67^{phox} (Fig. 5*B*) and the cells transfected with p41^{nox} and p67^{phox} (data not shown). In contrast, the cells expressing both p47^{phox} and p51^{nox} only marginally produced superoxide, when simulated with PMA (data not shown). Thus, p41^{nox} likely functions in combination with p51^{nox} as well as with p67^{phox} in activation of the phagocyte oxidase gp91^{phox}.

Activation of gp91^{phox}/Nox2 by p41^{nox} and p51^{nox} in COS-7 Cells—It has recently been reported that the monkey kidney COS-7 cells are useful for functional reconstitution of the phagocyte NADPH oxidase system at the cellular level (50). As expected, superoxide was produced in response to PMA by COS-7 cells transfected simultaneously with pcDNA3.0-gp91^{phox}, pEF-BOS-p47^{phox}, and pEF-BOS-p67^{phox} (Fig. 6). The superoxide production was not observed when cells were transfected with the gp91^{phox} cDNA alone or with solely the p47^{phox} and p67^{phox} cDNA (data not shown). These findings indicate that the phagocyte oxidase is successfully reconstituted in COS-7 cells. We next coexpressed gp91^{phox} with a pair of p41^{nox} and p51^{nox} in COS-7 cells, instead of a pair of p47^{phox} and p67^{phox}. Interestingly, the cells expressing the three proteins produced superoxide in the absence of any stimulants. The superoxide production was increased in response to PMA (Fig. 6). Furthermore, cells containing gp91^{phox}, p41^{nox}, and p67^{phox} also generated superoxide spontaneously, which was also enhanced by the addition of PMA (Fig. 6). On the other hand, gp91^{phox} was marginally activated by a pair of p47^{phox} and p51^{nox}, even when cells were stimulated with PMA (Fig. 6).

Expression of mRNAs for p41^{nox} and p51^{nox}—We next studied expression of the NOXO1 and NOXA1 genes encoding p41^{nox} and p51^{nox}, respectively. To quantitatively compare the expression of the two genes among various human tissues, we performed real time PCR analyses. As shown in Fig. 7*A*, the mRNA for p41^{nox} was abundant in colon and testis and also present in tissues such as pancreas, liver, thymus, and small intestine, but to a lesser extent. The p51^{nox} mRNA abundantly existed in pancreas; it was less but significantly expressed in liver, kidney, spleen, prostate, small intestine, and colon. Intriguingly, both mRNAs occurred together in several tissues, including colon, small intestine, liver, and pancreas (Fig. 7*B*). On the other hand, the NOX1 mRNA was most predominantly expressed in colon among adult tissues tested (Fig. 7*C*), which is in agreement with previous findings by other groups (10, 11, 14).

The NOXO1 and NOXA1 genes appear to be expressed solely in restricted cells of the tissues or at a low level in most cells, since detection of the PCR products for the two genes in any tissues required much more PCR cycles than that for the NOX1 gene (data not shown). Essentially the same patterns of tissue expression of the p51^{nox} and p41^{nox} genes were observed by Northern blot analysis (data not shown), although only weak signals could be obtained, which is consistent with the results of the PCR detection as mentioned above.

Activation of Nox1 by p41^{nox} and p51^{nox} in HEK293 and COS-7 Cells—Expression of both p41^{nox} and p51^{nox} in human colon suggests that they may be involved in activation of the Nox1 oxidase, which is abundantly present in this organ (Fig. 7). To test this possibility, we transfected the human embryonic kidney HEK293 cells with pcDNA3.0-Nox1, pEF-BOS-p41^{nox}, and pEF-BOS-p51^{nox}. As shown in Fig. 8*A*, cells cotransfected with all the three plasmids produced superoxide without any stimulants added. On the other hand, the production was not observed in cells that were individually transfected with Nox1, p41^{nox}, or p51^{nox} (data not shown) or in cells expressing both p41^{nox} and p51^{nox} but not Nox1 (Fig. 8*A*). Since p41^{nox} and p51^{nox} are adaptor proteins without any known catalytic domains, as shown here, it is conceivable that superoxide is directly produced by Nox1. This proposal is supported by the observation that superoxide production is almost completely blocked by treatment of the cells with 5 μM diphenylene iodo-

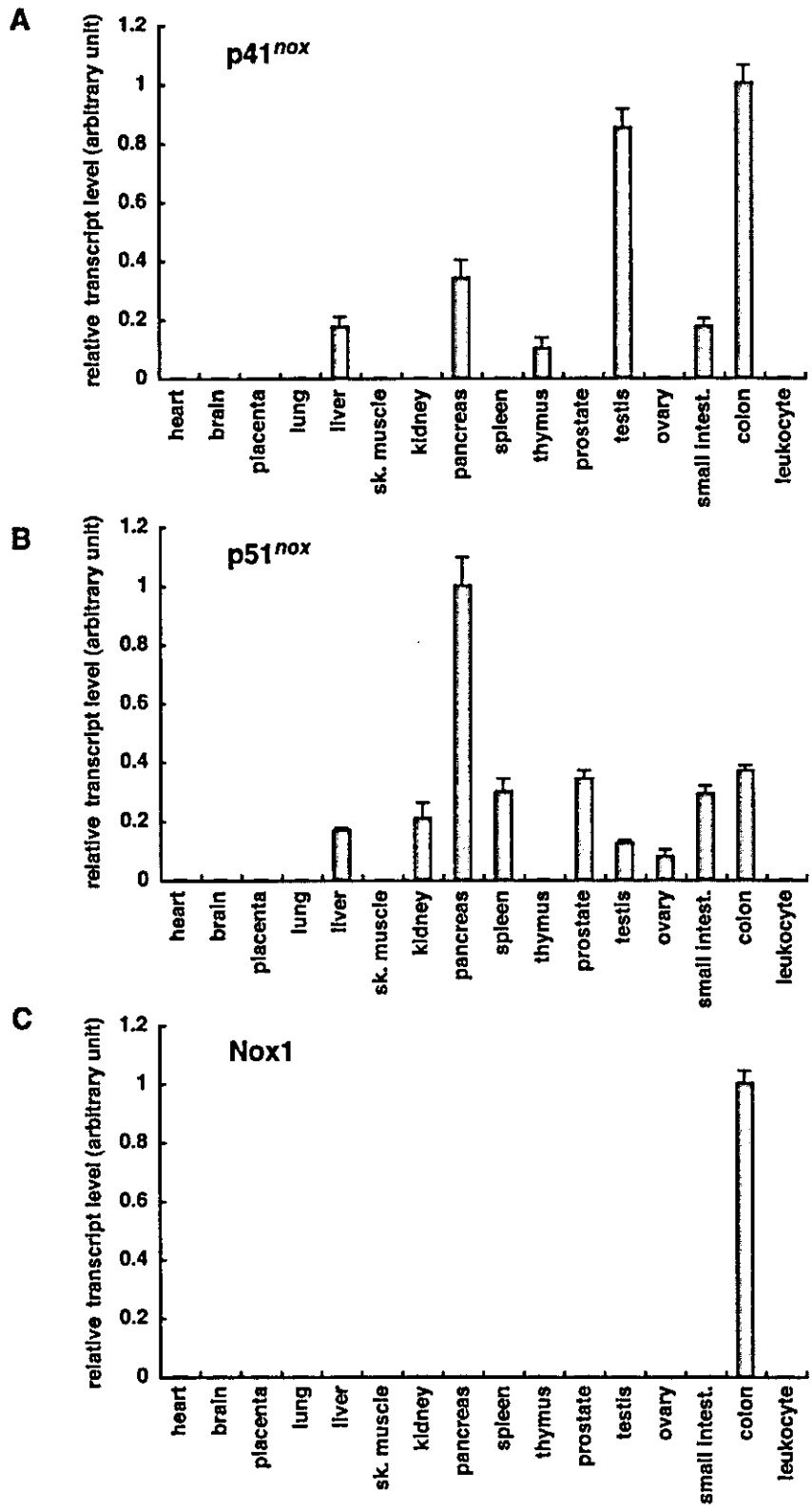

FIG. 7. **Expression of p41^{nox}, p51^{nox}, and Nox1 in human tissues.** The expression levels of mRNAs for the NOXO1, NOXA1, and NOX1 genes encoding p41^{nox} (*A*), p51^{nox} (*B*), and Nox1 (*C*), respectively, were analyzed by real time PCR using Human Multiple Tissue cDNA panels (Clontech). *sk. muscle*, skeletal muscle; *small intest.*, small intestine. Each *graph* represents the mean of the content of the indicated transcript normalized to glyceraldehyde-3-phosphate dehydrogenase content in triplicate samples, with *bars* representing the S.D. For details, see "Experimental Procedures."

nium, an inhibitor of the Nox family oxidases (data not shown). The superoxide production by Nox1 was enhanced by the addition of PMA (Fig. 8*A*).

To confirm that Nox1 can be activated by a pair of p41^{nox} and p51^{nox}, we next used COS-7 cells. Coexpression of Nox1 with both p41^{nox} and p51^{nox} in these cells also resulted in a constitutive production of superoxide (Fig. 8*B*). The addition of PMA to these cells increased the superoxide production, consistent with the results of the experiments using HEK293 cells (Fig. 8*A*). These findings indicate that p41^{nox} and p51^{nox} support activation of Nox1; activation appears to be partially constitutive.

We further tested the effect of other pairs of the p47^{phox} and p67^{phox} homologues in activation of Nox1. In the COS-7 cells where Nox1 was coexpressed with a pair of p41^{nox} and p67^{phox}, production was produced without stimuli, and the production was facilitated upon stimulation with PMA (Fig. 8*B*). Although Nox1 was normally inactive in cells that expressed both p47^{phox}

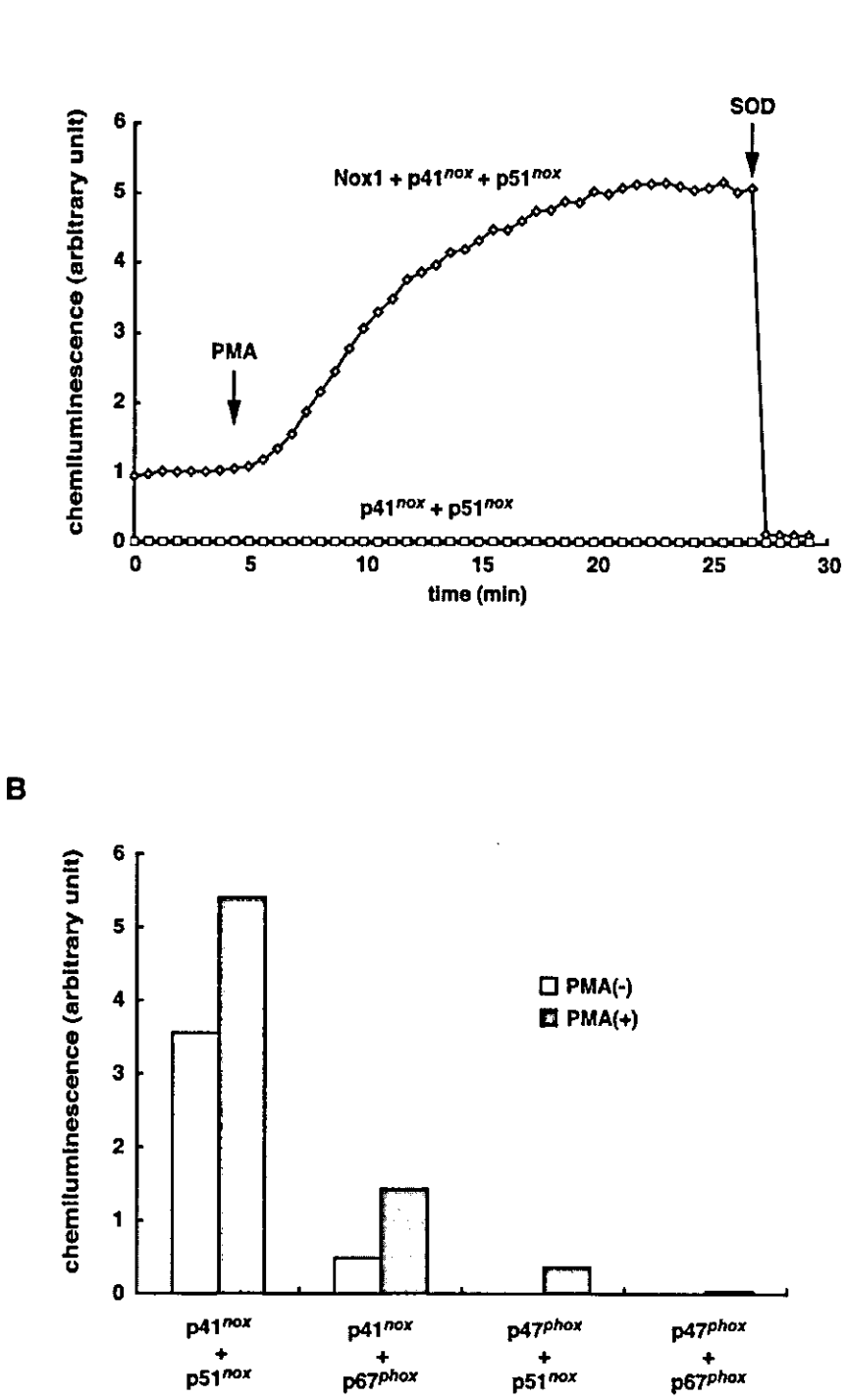

FIG. 8. **Effects of p41^{nox} and p51^{nox} on activation of Nox1 in HEK293 and COS-7 cells.** *A*, HEK293 cells were transfected simultaneously with pcDNA3.0-Nox1, pEF-BOS-p41^{nox}, and pEF-BOS-p51^{nox} or with pcDNA3.0 alone, pEF-BOS-p41^{nox}, and pEF-BOS-p51^{nox}. The transfected cells (1×10^5 cells) were incubated for 5 min at 37 °C and then stimulated with PMA (200 ng/ml). Chemiluminescence change was continuously monitored with DIOGENES, and SOD (50 μg/ml) was added where indicated. For details, see "Experimental Procedures." The experiments have been repeated more than three times with similar results. *B*, COS-7 cells were transfected simultaneously with pcDNA3.0-Nox1 and the following pair of pEF-BOS vectors encoding the oxidase organizer and activator homologues: p41^{nox} and p51^{nox}; p41^{nox} and p67^{phox}; p47^{phox} and p51^{nox}; or p47^{phox} and p67^{phox}. The transfected cells (1×10^5 cells) were incubated for 5 min at 37 °C and then stimulated with PMA (200 ng/ml). Chemiluminescence change was continuously monitored with DIOGENES. Superoxide production is expressed as the percentage of activity relative to control cells transfected with pcDNA3.0-Nox1, pEF-BOS-p41^{nox}, and pEF-BOS-p51^{nox}. Each *graph* represents the mean of data from three independent transfections.

and p51^{nox}, the oxidase became active in response to PMA. Thus, stimulus-independent production of superoxide occurred only when p41^{nox} was present instead of p47^{phox}. On the other hand, Nox1 could not be activated either with or without stimuli by a pair of the classical homologues p47^{phox} and p67^{phox} under the present conditions.

Effect of p22^{phox} on Nox1-dependent Superoxide Production—It is well established that gp91^{phox} tightly associates with p22^{phox} in phagocytes, whereas it has remained unclear whether Nox1 is also capable of forming a complex with p22^{phox}. To address this question, we tested the effect of expression of p22^{phox} on Nox1-dependent superoxide production. For this purpose, we used CHO cells, since it has been reported that CHO cells scarcely express the mRNA of p22^{phox} (53). The p22^{phox} mRNA is known to be present in a wide variety of cells (14); COS-7 and HEK293 cells used in the present study indeed expressed a significant amount of the p22^{phox} mRNA, which is consistent with the observation that transfection of these cells with the p22^{phox} cDNA was not required for the gp91^{phox} activity (Fig. 6; data not shown). As expected, gp91^{phox} was almost dormant in CHO cells cotransfected with the p41^{nox} and p51^{nox} cDNAs but not with the p22^{phox} cDNA, even when cells were stimulated with PMA (Fig. 9*A*). Simultaneous transfection with gp91^{phox} and p22^{phox} led to superoxide production in CHO cells expressing both p41^{nox} and p51^{nox}, a production that was facilitated upon cell stimulation with PMA (Fig. 9*A*). When Nox1 was expressed in CHO cells instead of gp91^{phox} under these conditions, a small amount of superoxide was produced

without cotransfection with the p22^{phox} cDNA (Fig. 9*B*). Treatment of cells with PMA slightly increased the Nox1-dependent superoxide production. Intriguingly, coexpression of p22^{phox} culminated in a great enhancement of superoxide production by Nox1, either with or without PMA stimulation (Fig. 9*B*). These findings suggest that Nox1 can be complexed with p22^{phox}.

DISCUSSION

In this study, we have identified novel functional homologues of the phagocyte oxidase proteins p47^{phox} and p67^{phox}, tentatively designated p41^{nox} (the NOXO1 gene product) and p51^{nox} (the NOXA1 gene product), respectively. The homologues retain most of the functional modules for protein-protein interactions: the SH3 domains of p41^{nox} interact with p22^{phox}; p41^{nox}, as well as p47^{phox}, binds to p51^{nox} and p67^{phox} via a tail-to-tail interaction; and the N-terminal TPR domain of p51^{nox} interacts with Rac in a GTP-bound state. Consistent with the conservation of the crucial interactions between oxidase factors, p41^{nox} and p51^{nox} function together or in combination with a classical one to support superoxide production by the phagocyte NADPH oxidase. We also show that Nox1 also can be activated by the novel homologues, a finding that will help our understanding of the regulation of Nox1. During the completion of the present study, Bánfi *et al.* (54) have reported the cloning of mouse NOXO1 and NOXA1 and shown that they are capable of activating Nox1.

Activation of the phagocyte NADPH oxidase gp91^{phox} is known to require, as a switch, at least two events elicited during intracellular signal transduction in stimulated cells. One of the events is a conformational change of p47^{phox}. The SH3 domains of p47^{phox} are normally masked via an intramolecular interaction with the AIR; upon cell stimulation, p47^{phox} is phosphorylated, which leads to its conformational change that allows the domains to become accessible to p22^{phox}. The resultant interaction between p47^{phox} and p22^{phox} plays an essential role in the oxidase activation (20–22). The other crucial event is conversion of Rac to the active state; only the GTP-bound Rac, but not the GDP-bound one, binds to p67^{phox}, thereby activating the phagocyte oxidase. In resting phagocytes, both switches are kept "off," preventing the oxidase from producing superoxide. In contrast, the present findings have demonstrated that novel homologues of p47^{phox} and p67^{phox} can activate gp91^{phox} and Nox1 without cell stimulation under certain conditions (Figs. 6 and 8). In COS-7 cells expressing a pair of p41^{nox} and p51^{nox} or a pair of p41^{nox} and p67^{phox}, gp91^{phox} seems to be constitutively active, albeit not in a state fully activated (Fig. 6). On the other hand, PMA is absolutely required for activation of gp91^{phox} in cells that contain both p47^{phox} and p67^{phox} (Fig. 6). Similarly, Nox1 spontaneously generated superoxide when it was cotransfected in COS-7 cells with both cDNAs for p41^{nox} and p51^{nox} or with those for p41^{nox} and p67^{phox} (Fig. 8). In the presence of p47^{phox} and p51^{nox}, however, activation of this oxidase completely depends on the addition of PMA as a stimulant (Fig. 8).

Thus stimulus-independent activation of Nox1 and gp91^{phox} seems to require p41^{nox}. On the other hand, Nox1 and gp91^{phox} are both dormant in cells expressing p47^{phox} instead of p41^{nox}, but become activated in response to PMA. In this context, it should be noted that p41^{nox} does not harbor a region homologous to the AIR that prevents the SH3 domains of p47^{phox} from interacting with p22^{phox} (Fig. 1). Indeed, the SH3 domains of p41^{nox} are considered to be in a state accessible to its target, since full-length p41^{nox} binds to p22^{phox} (Fig. 3). On the other hand, full-length p47^{phox} is incapable of interacting with p22^{phox} under the conditions where its isolated SH3 domains fully associate with the target (Fig. 3). It is thus likely that

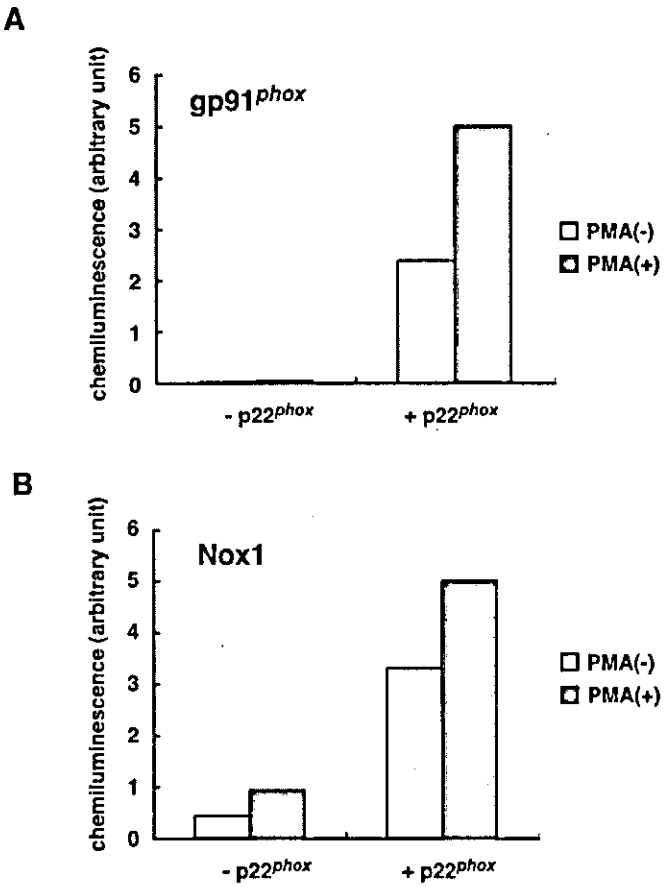

FIG. 9. **Effect of p22^{phox} on gp91^{phox}- and Nox1-dependent superoxide production in CHO cells expressing both p41^{nox} and p51^{nox}.** *A*, CHO cells were transfected simultaneously with pcDNA3.0-gp91^{phox}, pEF-BOS-p41^{nox}, and pEF-BOS-p51^{nox} or with pcDNA3.0-gp91^{phox}, pEF-BOS-p41^{nox}, pEF-BOS-p51^{nox}, and pEF-BOS-p22^{phox}. The transfected cells (1×10^5 cells) were incubated for 5 min at 37 °C and then stimulated with PMA (200 ng/ml). Chemiluminescence change was continuously monitored with DIOGENES. Superoxide production is expressed as the percentage of activity relative to control cells transfected with pcDNA3.0-gp91^{phox}, pEF-BOS-p41^{nox}, pEF-BOS-p51^{nox}, and pEF-BOS-p22^{phox}. Each *graph* represents the mean of data from three independent transfections. *B*, CHO cells were transfected simultaneously with pcDNA3.0-Nox1, pEF-BOS-p41^{nox}, and pEF-BOS-p51^{nox} or with pcDNA3.0- Nox1, pEF-BOS-p41^{nox}, pEF-BOS-p51^{nox}, and pEF-BOS-p22^{phox}. The transfected cells (1×10^5 cells) were incubated for 5 min at 37 °C and then stimulated with PMA (200 ng/ml). Chemiluminescence change was continuously monitored with DIOGENES. Superoxide production is expressed as the percentage of activity relative to control cells transfected with pcDNA3.0-Nox1, pEF-BOS-p41^{nox}, pEF-BOS-p51^{nox}, and pEF-BOS-p22^{phox}. Each *graph* represents the mean of data from three independent transfections.

p41^{nox} occurs in a constitutively active form, whereas p47^{phox} is normally inactive but becomes accessible to p22^{phox} via the stimulus-induced conformational change. The difference may explain the reason why p41^{nox} is more active than p47^{phox} even in activation of gp91^{phox} (Figs. 5*A* and 6) and Nox1 (Fig. 8*B*), since it seems very unlikely that all of the p47^{phox} molecules become activated at the same time in cells; it is well known that only a part (about 10%) of p47^{phox} translocates to the membrane when neutrophils are stimulated with PMA, one of the most potent activators of the phagocyte oxidase *in vivo* (3–9).

The present study suggests that Nox1 also forms a heterodimer with p22^{phox} as gp91^{phox}/Nox2 does (Fig. 9). In CHO cells containing p41^{nox} and p51^{nox}, stimulus-independent superoxide production by Nox1 is greatly enhanced by ectopic expression of p22^{phox} (Fig. 9). This finding supports the above mentioned hypothesis that p41^{nox} functions, via binding to

p22^{phox} without stimulation, in constitutive activation of Nox1. Whereas gp91^{phox} is almost inactive in CHO cells that are not transfected with the cDNA of p22^{phox}, Nox1 can produce a small amount of superoxide without the transfection (Fig. 9). The reason for the difference is currently unknown. It may be possible that Nox1 interacts with p22^{phox} with a much higher affinity than does gp91^{phox} if there is a trace, undetectable amount of p22^{phox} in CHO cells. It seems also possible that Nox1 might be complexed with a heretofore unidentified homologue of p22^{phox} in CHO cells. This question should be addressed in the future studies.

In addition to the difference between p41^{nox} and p47^{phox}, the regulation of p51^{nox} also does not seem to be the same as that of its homologue p67^{phox}. We have recently shown that p40^{phox} enhances the phagocyte oxidase activation by facilitating the membrane translocation of p67^{phox} and p47^{phox} and that this effect is totally dependent on the interaction of p40^{phox} with p67^{phox} (40). Since p51^{nox} is incapable of interacting with p40^{phox} (Fig. 4), the regulation mediated via p40^{phox} cannot be expected in an activation system involving p51^{nox}. Although the target protein for the N-terminal SH3 domain of p67^{phox}, the most conserved module of this protein (55), still remains unidentified, the absence of this domain in p51^{nox} may suggest a difference in oxidase activation between the homologues.

Activation of gp91^{phox} by p41^{nox} and p51^{nox} in K562 cells is entirely dependent on stimulation with PMA (Fig. 5), whereas, even without the addition of any stimulants, gp91^{phox} can produce superoxide in COS-7 cells containing p41^{nox} and p51^{nox} (Fig. 6). The reason for this discrepancy is presently unknown. One possible explanation is that the state of Rac, a switch of the oxidase activation, may be different between types of cells; for instance, the amount of GTP-bound Rac might be higher in COS-7 cells than K562 cells. In the presence of GTP-bound Rac, a rate-limiting step will be the conformational change of p47^{phox}, another switch of the oxidase activation; thus, PMA is still required in COS-7 cells with p47^{phox} but not in ones with the constitutively active homologue p41^{nox} (Fig. 6). Even in the latter case, the amount of GTP-bound Rac may be insufficient, because superoxide production is enhanced by the addition of PMA (Fig. 6). This stimulant is known to facilitate the formation of GTP-bound Rac at the cellular level (56). It is also possible that, in K562 cells, p41^{nox} is kept in an inactive state by an unknown mechanism.

In summary, the present study demonstrates that distinct pairs of the novel and classical homologues of p47^{phox} and p67^{phox} are capable of supporting activation of gp91^{phox}/Nox2 and Nox1, suggesting the existence of a common mechanism underlying the activation of Nox family oxidases. Future studies should clarify whether other Nox oxidases such as Nox4 are similarly regulated or not. In addition to the common features of the homologues of p47^{phox} and p67^{phox}, there are also differences between them in regulation of Nox oxidases. First, gp91^{phox} likely prefers p67^{phox} to p51^{nox} as its activator (Fig. 6). In contrast, p51^{nox} appears to activate Nox1 more efficiently than p67^{phox} (Fig. 8). Second, distinct types of regulation for Nox oxidases are considered to be achieved by different combinations of the oxidase organizers p47^{phox} and p41^{nox} with the oxidase activators p67^{phox} and p51^{nox}; a phosphorylation-induced conformational change of p47^{phox} upon cell stimulation serves as a switch to activate the oxidase, whereas p41^{nox} seems to be constitutively in an active state; p67^{phox}, but not p51^{nox}, can regulate the oxidase activation in cooperation with p40^{phox}. Thus, a certain Nox oxidase can be regulated in a manner dependent on the oxidase factors expressed in cells. For example, since p41^{nox} and p51^{nox}, as well as Nox1, are expressed in the colon, Nox1 is mainly controlled by the two novel homologues in this organ. The present findings suggest that the active oxidase complex in the colon comprises Nox1, p22^{phox}, p41^{nox}, p51^{nox}, and Rac: Nox1 is likely complexed with p22^{phox} at the membrane (Fig. 9); p41^{nox} constitutively associates with the Nox1-p22^{phox} complex via direct binding to p22^{phox} (Fig. 3); and p51^{nox} directly interacts with Rac and p41^{nox} via the N-terminal TPR domain (Fig. 4) and the SH3 domain at the C terminus (Fig. 3), respectively. On the other hand, it is known that vascular smooth muscle cells express Nox1 (57) and produce superoxide in a stimulus-dependent manner (37). As expected from the dependence, p47^{phox} exists in the cells and plays a crucial role in superoxide production (58), whereas the cells do not contain p67^{phox} (37), raising the possibility that p51^{nox} may be present instead.

Acknowledgment—We are grateful to Yohko Kage (Kyushu University) for technical assistance.

REFERENCES

1. Lambeth, J. D., Cheng, G., Arnold, R. S., and Edens, W. E. (2000) *Trends Biochem. Sci.* **25,** 459–461
2. Lambeth, J. D. (2002) *Curr. Opin. Hematol.* **9,** 11–17
3. DeLeo, F. R., and Quinn, M. T. (1996) *J. Leukocyte Biol.* **60,** 677–691
4. Babior, B. M. (1999) *Blood* **93,** 1464–1476
5. Nauseef, W. M. (1999) *Proc. Assoc. Am. Physicians* **111,** 373–382
6. Clark, R. A. (1999) *J. Infect. Dis.* **179,** Suppl. 2, S309–S317
7. Bokoch, G. M., and Diebold, B. A. (2002) *Blood* **100,** 2692–2696
8. Sumimoto, H., Ito, T., Hata, K., Mizuki, K., Nakamura, R., Kage, Y., Sakaki, Y., Nakamura, M., and Takeshige, K. (1997) in *Membrane Proteins: Structure, Function, and Expression Control* (Hamasaki, N., and Mihara, K., eds) pp. 235–245, Kyushu University Press, Fukuoka, Japan
9. Roos, D., de Boer, M., Kuribayashi, F., Meischl, C., Weening, R. S., Segal, A. W., Åhlin, A., Nemet, K., Hossle, J. P., Bernatowska-Matuszkiewicz, E., and Middleton-Price, H. (1996) *Blood* **87,** 1663–1681
10. Suh, Y. A., Arnold, R. S., Lassegue, B., Shi, J., Xu, X., Sorescu, D., Chung, A. B., Griendling, K. K., Lambeth, J. D. (1999) *Nature* **401,** 79–82
11. Bánfi, B., Maturana, A., Jaconi, S., Arnaudeau, S., Laforge, T., Sinha, B., Ligeti, E., Demaurex, N., Krause, K.-H. (2000) *Science* **287,** 138–142
12. Geiszt, M., Kopp, J. B., Várnai, P., and Leto, T. L. (2000) *Proc. Natl. Acad. Sci. U. S. A.* **97,** 8010–8014
13. Shiose, A., Kuroda, J., Tsuruya, K., Hirai, M., Hirakata, H., Naito, S., Hattori, M., Sakaki, Y., and Sumimoto, H. (2001) *J. Biol. Chem.* **276,** 1417–1423
14. Cheng, G., Cao, Z., Xu, X., van Meir, E. G., and Lambeth, J. D. (2001) *Gene (Amst.)* **269,** 131–140
15. Heyworth, P. G., Curnutte, J. T., Nauseef, W. M., Volpp, B. D., Pearson, D. W., Rosen, H., and Clark, R. A. (1991) *J. Clin. Invest.* **87,** 352–356
16. Dusi, S., Donini, M., and Rossi, F. (1996) *Biochem. J.* **314,** 409–412
17. Finan, P., Shimizu, Y., Gout, I., Hsuan, J., Truong, O., Butcher, C., Bennett, P., Waterfield, M. D., and Kellie, S. (1994) *J. Biol. Chem.* **269,** 13752–13755
18. Leusen, J. H., Fluiter, K., Hilarius, P. M., Roos, D., Verhoeven, A. J., and Bolscher, B. G. (1995) *J. Biol. Chem.* **270,** 11216–11221
19. Kami, K., Takeya, R., Sumimoto, H., and Kohda, D. (2002) *EMBO J.* **21,** 4268–4276
20. Sumimoto, H., Kage, Y., Nunoi, H., Sasaki, H., Nose, T., Fukumaki, Y., Ohno, M., Minakami, S., and Takeshige, K. (1994) *Proc. Natl. Acad. Sci. U. S. A.* **91,** 5345–5349
21. Leto, T. L., Adams, A. G., and de Mendez, I. (1994) *Proc. Natl. Acad. Sci. U. S. A.* **91,** 10650–10654
22. Ago, T., Nunoi, H., Ito, T., and Sumimoto, H. (1999) *J. Biol. Chem.* **274,** 33644–33653
23. Rotrosen, D., and Leto, T. L. (1990) *J. Biol. Chem.* **265,** 19910–19915
24. El Benna, J., Faust, L. P., and Babior, B. M. (1994) *J. Biol. Chem.* **269,** 23431–23436
25. Huang, J., and Kleinberg, M. E. (1999) *J. Biol. Chem.* **274,** 19731–19737
26. Shiose, A., and Sumimoto, H. (2000) *J. Biol. Chem.* **275,** 13793–13801
27. Heyworth, P. G., Bohl, B. P., Bokoch, G. M., and Curnutte, J. T. (1994) *J. Biol. Chem.* **269,** 30749–30752
28. Koga, H., Terasawa, H., Nunoi, H., Takeshige, K., Inagaki, F., and Sumimoto, H. (1999) *J. Biol. Chem.* **274,** 25051–25060
29. Lapouge, K., Smith, S. J. M., Walker, P. A., Gamblin, S. J., Smerdon, S. J., and Rittinger, K. (2000) *Mol. Cell* **6,** 899–907
30. Nisimoto, Y., Motalebi, S., Han, C.-H., and Lambeth, J. D. (1999) *J. Biol. Chem.* **274,** 22999–23005
31. Diebold, B. A., and Bokoch, G. M. (2001) *Nat. Immunol.* **2,** 211–215
32. Dang, P. M., Cross, A. R., and Babior, B. M. (2001) *Proc. Natl. Acad. Sci. U. S. A.* **98,** 3001–3005
33. Gorzalczany, Y., Alloul, N., Sigal, N., Weinbaum, C., and Pick, E. (2002) *J. Biol. Chem.* **277,** 18605–18610
34. Freeman, J. L., and Lambeth, J. D. (1996) *J. Biol. Chem.* **271,** 22578–22582
35. Koshkin, V., Lotan, O., and Pick, E. (1996) *J. Biol. Chem.* **271,** 30326–30329
36. Bánfi, B., Molnár, G., Maturana, A., Steger, K., Hegedûs, B., Demaurex, N., Krause, K.-H. (2001) *J. Biol. Chem.* **276,** 37594–37601
37. Patterson, C., Ruef, J., Madamanchi, N. R., Barry-Lane, P, Hu, Z., Horaist, C., Ballinger, C. A., Brasier, A. R., Bode, C., and Runge, M. S. (1999) *J. Biol. Chem.* **274,** 19814–19822
38. Griendling, K. K., and Ushio-Fukai, M. (1997) *Trends Cardiovasc. Med.* **7,** 301–307

39. Brar, S. S., Kennedy, T. P., Sturrock, A. B., Huecksteadt, T. P., Quinn, M. T., Whorton, A. R., and Hoidal, J. R. (2002) *Am. J. Physiol.* **282,** C1212–C1224
40. Kuribayashi, F., Nunoi, N., Wakamatsu, K., Tsunawaki, S., Sato, K., Ito, T., and Sumimoto, H. (2002) *EMBO J.* **21,** 6312–6320
41. Mizushima, S., and Nagata, S. (1990) *Nucleic Acids Res.* **18,** 5322
42. Noda, Y., Takeya, R., Ohno, S., Naito, S., Ito, T., and Sumimoto, H. (2001) *Genes Cells* **6,** 107–119
43. Kohjima, M., Noda, Y., Takeya, R., Saito, N., Takeuchi, K., and Sumimoto, H. (2002) *Biochem. Biophys. Res. Commun.* **299,** 641–646
44. Johnson, M. R., Wang, K., Smith, J. B., Heslin, M. J., and Diasio, R. B. (2000) *Anal. Biochem.* **278,** 175–184
45. Hiroaki, H., Ago, T., Ito, T., Sumimoto, H., and Kohda, D. (2001) *Nat. Struct. Biol.* **6,** 526–530
46. Ago, T., Kuribayashi, F., Hiroaki, H., Takeya, R., Ito, T., Kohda, D., and Sumimoto, H. (2003) *Proc. Natl. Acad. Sci. U. S. A.* **100,** 4474–4479
47. Ito, T., Matsui, Y., Ago, T., Ota, K., and Sumimoto, H. (2001) *EMBO J.* **20,** 3938–3946
48. Hata, K., Takeshige, K., and Sumimoto, H. (1997) *Biochem. Biophys. Res. Commun.* **241,** 226–231
49. Han, C.-H., Freeman, J. L. R., Lee, T., Motalebi, S. A., and Lambeth, J. D. (1998) *J. Biol. Chem.* **273,** 16663–16668
50. Price, M. O., McPhail, L. C., Lambeth, J. D., Han, C.-H., Knaus, U. G., and Dinauer, M. C. (2002) *Blood* **99,** 2653–2661
51. Dinauer, M. C., Pierce, E. A., Erickson, R. W., Muhlebach, T. J., Messner, H., Orkin, S. H., Seger, R. A., and Curnutte, J. T. (1991) *Proc. Natl. Acad. Sci. U. S. A.* **88,** 11231–11235
52. Leusen, J. H. W., Bolscher, B. G. J. M., Hilarius, P. M., Weening, R. S., Kaulfersch, W., Segar, R. A., Roos, D., and Verhoeven, A. J. (1994) *J. Exp. Med.* **180,** 2329–2334
53. Biberstine-Kinkade, K. J., Yu, L., Stull, N., LeRoy, B., Bennett, S., Cross, A., and Dinauer, M. C. (2002) *J. Biol. Chem.* **277,** 30368–30374
54. Bánfi, B., Clark, R. A., Steger, K., and Krause, K.-H. (2003) *J. Biol. Chem.* **278,** 3510–3513
55. Mizuki, K., Kadomatsu, K., Hata, K., Ito, T., Fan, Q.-W., Kage, Y., Fukumaki, Y., Sakaki, Y., Takeshige, K., and Sumimoto, H. (1998) *Eur. J. Biochem.* **251,** 573–582
56. Akasaki, T., Koga, H., and Sumimoto, H. (1999) *J. Biol. Chem.* **274,** 18055–18059
57. Lassègue, B., Sorescu, D., Szöcs, K., Yin, Q., Akers, M., Zhang, Y., Grant, S. L., Lambeth, J. D., and Griendling, K. K. (2001) *Circ. Res.* **88,** 888–894
58. Lavigne, M. C., Malech, H. L., Holland, S. M., and Leto, T. L. (2001) *Circulation* **104,** 79–84

PI3K and Btk differentially regulate B cell antigen receptor-mediated signal transduction

Harumi Suzuki[1*†], Satoshi Matsuda[1,2*], Yasuo Terauchi[2,3], Mari Fujiwara[1,2], Toshiaki Ohteki[1‡], Tomoichiro Asano[3], Timothy W. Behrens[4], Taku Kouro[5], Kiyoshi Takatsu[5], Takashi Kadowaki[2,3] and Shigeo Koyasu[1,2]

Published online 3 February 2003; doi:10.1038/ni890

Phosphoinositide-3 kinase (PI3K) is thought to activate the tyrosine kinase Btk. However, through analysis of PI3K$^{-/-}$ and Btk$^{-/-}$ mice, B cell antigen receptor (BCR)-induced activation of Btk in mouse B cells was found to be unaffected by PI3K inhibitors or by a lack of PI3K. Consistent with this observation, PI3K$^{-/-}$ Btk$^{-/-}$ double-deficient mice had more severe defects than either single-mutant mouse. NF-κB activation along with Bcl-x$_L$ and cyclin D2 induction were severely blocked in both PI3K$^{-/-}$ and Btk$^{-/-}$ single-deficient B cells. Transgenic expression of Bcl-x$_L$ restored the development and BCR-induced proliferation of B cells in PI3K$^{-/-}$ mice. Our results indicate that PI3K and Btk have unique roles in proximal BCR signaling and that they have a common target further downstream in the activation of NF-κB.

Phosphoinositide-3 kinase (PI3K) is a key enzyme producing phospholipid second messengers and has an important role in various signal transduction pathways[1,2]. PI3K family members are classified into three groups according to their structure and substrate specificity[2]. Among them, class I$_A$ heterodimeric PI3Ks consisting of a catalytic subunit (p110α, p110β, p110δ) and a regulatory subunit (p85α, p85β, p55γ) are involved in receptor-mediated signaling in the immune system. To precisely examine the functions of class I$_A$ PI3Ks, we and others generated PI3K$^{-/-}$ mice deficient for the gene encoding p85α, the most abundantly and ubiquitously expressed regulatory subunit of class I$_A$ PI3Ks[3–5]. Due to alternative splicing, p55α and p50α, in addition to p85α, are produced from the same gene[6,7]. Mice lacking only p85α (used here as PI3K$^{-/-}$ mice) are viable[3,4], whereas mice lacking all alternatively spliced products are unable to survive after birth[5]. In the absence of PI3K, B cell development from pro-B cells to pre-B cells in the bone marrow is impaired and the number of mature B cells in the periphery is decreased[4,5]. In addition, mature B cell functions such as mitogen-induced proliferation *in vitro* are severely impaired[4].

Crosslinking of the surface B cell antigen receptor (BCR) evokes sequential activation of a variety of protein and lipid kinases including Src family kinases (Lyn, Fyn, Blk), Syk, Btk, Akt (also known as PKB) and PI3K[2,8–12]. Although activation of PI3K is observed upon BCR stimulation, signaling events upstream and downstream of PI3K are not well characterized. In B cells, Lyn, c-Cbl, CD19 and BCAP bind the p85α subunit of PI3K, suggesting that these molecules are upstream activators of PI3K. On the other hand, various proteins containing pleckstrin homology (PH) domains, such as Akt, phosphoinositide-dependent kinase 1 (PDK1) and Btk, are thought to function downstream of PI3K, because of the ability of their PH domains to bind phosphatidylinositol-(3,4)-bisphosphate (PIP$_2$) or phosphatidylinositol-(3,4,5)-trisphosphate (PIP$_3$), products of PI3K[13,14].

Btk, a Tec family kinase, is activated by tyrosine phosphorylation and has a critical role in BCR signaling[12,15–18]. Btk$^{-/-}$ mice, as well as mice with the *Xid* mutation (a natural mutation in the PH domain of Btk in which an arginine residue critical for the binding to PIP$_3$ is replaced by cysteine), show deficiencies in the development and activation of B cells. In humans, deficiency of Btk leads to X-linked Bruton's type agammaglobulinemia (XLA)[12,15,16]. Stimulation-dependent membrane localization of a Btk-PH domain-GFP chimeric protein in transient transfection systems has been demonstrated and such membrane recruitment is blocked by wortmannin, a PI3K inhibitor[19,20]. Overexpression of the p110 PI3K catalytic subunit in a B cell line results in Btk tyrosine phosphorylation[21]. It has been proposed from these observations that PI3K is responsible for the activation of Btk by bringing Btk to the plasma membrane through interactions between the PH domain of Btk and PIP$_3$[13,14], leading to tyrosine phosphorylation of Btk by other protein tyrosine kinases such as Syk. It was thus not surprising that PI3K$^{-/-}$ mice show a phenotype similar to that of Btk$^{-/-}$ or *Xid* mice[4,5].

[1]*Department of Microbiology and Immunology, Keio University School of Medicine, Tokyo 160-8582, Japan.* [2]*Core Research for Evolutional Science and Technology (CREST), Japan Science and Technology Corporation (JST), Kawaguchi 332-0012, Japan.* [3]*Department of Metabolic Diseases, Graduate School of Medicine, University of Tokyo, Tokyo 113-8655, Japan.* [4]*Department of Medicine, Center for Immunology, University of Minnesota, Minneapolis, MN 55455, USA.* [5]*Department of Immunology, Institute of Medical Science, University of Tokyo, Tokyo 108-8639, Japan.* *These authors contributed equally to this work. †Present address: Department of Microbiology and Immunology, Yamaguchi University School of Medicine, Ube, Yamaguchi 755-8580, Japan.* ‡*Present address: Department of Parasitology, Akita University School of Medicine, Hondo, Akita 010-8543, Japan. Correspondence should be addressed to S.K. (koyasu@sc.itc.keio.ac.jp).*

BCR stimulation also activates the serine-threonine kinase Akt[2,22]. Akt has crucial roles in anti-apoptotic signal transduction as well as cell cycle progression[23–25]. Activation of Akt prevents apoptosis in many cell types and its anti-apoptotic effect is blocked by wortmannin. One product of PI3K, PIP_2, is reported to associate with the PH domain of Akt to recruit the enzyme to the plasma membrane. Similarly, another PI3K product, PIP_3, recruits PDK1, which phosphorylates Akt to activate its kinase activity. Akt is the major downstream target of PI3K in many signal transduction pathways[2,23–26].

Here, we further investigated the role of PI3K in B cell signal transduction pathways and the functional relationship between PI3K and Btk, using $PI3K^{-/-}$ and $Btk^{-/-}$ mice. Contrary to our expectations, BCR-induced activation of Btk was unaffected by the lack of PI3K or by PI3K inhibitors. On the other hand, BCR-induced activation of Akt was normal in $Btk^{-/-}$ B cells, but was severely impaired in $PI3K^{-/-}$ B cells. Furthermore, $PI3K^{-/-}Btk^{-/-}$ double-deficient mice show more severe phenotypes than either single-deficient mouse. These biochemical and genetic data show that PI3K and Btk function independently in BCR signal transduction pathways. Among downstream events, activation of NF-κB and induction of Bcl-x_L and cyclin D2 were impaired in both $PI3K^{-/-}$ and $Btk^{-/-}$ single-deficient B cells. Forced expression of Bcl-x_L restored development and proliferative responses of B cells in $PI3K^{-/-}$ mice. Our results indicate that class I_A PI3K and Btk have clearly distinct roles in BCR signal transduction.

Results

PI3K-dependent activation of Akt upon BCR stimulation

B cells from $PI3K^{-/-}$ mice used in this study expressed low amounts of p50α[4]. Expression of p85β and p55γ regulatory subunits was very low or undetectable in $PI3K^{-/-}$ and wild-type (WT) B cells (**Fig. 1a**). Expression of p110δ, the most abundantly expressed catalytic subunit in B cells, was reduced in the absence of these regulatory subunits (**Fig. 1a**). BCR-dependent activation of PI3K in the absence of p85α was examined by *in vitro* kinase assay, using phosphatidylinositol as a substrate to detect generation of phosphatidylinositol-3-phosphate (**Fig. 1b**). Total PI3K activity in tyrosine phosphorylated proteins was increased by BCR stimulation in WT and $Btk^{-/-}$ mice. In contrast, only a small amount of PI3K activity was observed upon BCR stimulation in $PI3K^{-/-}$ B cells (**Fig. 1b**; ~5% of WT activity), as previously reported[4]. The p50α regulatory subunit and possibly another class of PI3K likely contribute to this residual increase of PI3K activity in $PI3K^{-/-}$ B cells. On the contrary, activation of PI3K was unaffected in $Btk^{-/-}$ B cells.

Because Akt is widely accepted as a downstream target of PI3K in B cell signal transduction[2,22–26], we investigated BCR-mediated Akt activation by immunoblotting with specific monoclonal antibodies (mAbs) that detect phosphorylation at residues Thr^{308} and Ser^{473} of Akt, which is known to correlate with its kinase activity[27,28]. Phosphorylation of Akt on the Thr^{308} and Ser^{473} residues was increased upon BCR stimulation after 5 min in WT B cells, whereas phosphorylation of Akt

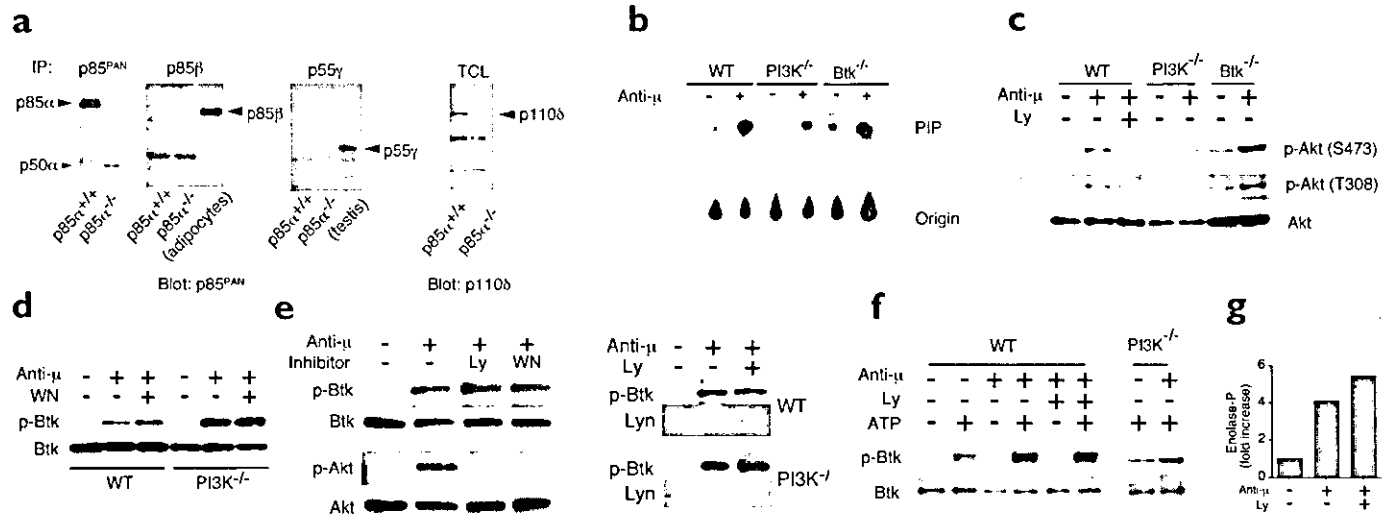

Figure 1. The Akt, but not the Btk, pathway is dependent on PI3K in B cells. (**a**) Expression of PI3K regulatory subunits in $PI3K^{-/-}$ ($p85\alpha^{-/-}$) and WT ($p85\alpha^{+/+}$) B cells. Postnuclear lysates of B cells derived from the indicated mice were immunoprecipitated with anti-$p85^{PAN}$ and specific antisera for p85β and p55γ, then immunoblotted with anti-$p85^{PAN}$. Adipocytes and testis were used as positive controls for p85β and p55γ, respectively. Or, total cell lysates (TCL) prepared from $PI3K^{-/-}$ ($p85\alpha^{-/-}$) and WT ($p85\alpha^{+/+}$) B cells were immunoblotted with anti-p110δ. (**b**) PI3K activities in $PI3K^{-/-}$, $Btk^{-/-}$ and WT B cells. PI3K activities from BCR-stimulated B cells of the indicated genotypes were assayed. (**c**) PI3K-dependent activation of Akt. BCR-mediated activation of Akt in $PI3K^{-/-}$ and $Btk^{-/-}$ B cells was evaluated by immunoblotting with a specific antibody detecting phosphorylation at Thr^{308} (p-Akt (T308)) and Ser^{473} (p-Akt (S473)) residues of Akt. Membranes were re-blotted with anti-Akt (Akt). Data are representative of four independent experiments with similar results. (**d**) BCR-induced tyrosine phosphorylation of Btk in $PI3K^{-/-}$ B cells. WT and $PI3K^{-/-}$ B cells on a BALB/c background were stimulated with anti-IgM $F(ab)'_2$ (Anti-μ) in the presence or absence of 25 nM wortmannin (WN). Btk was then immunoprecipitated by anti-Btk and immunoblotted with 4G10 (p-Btk). Membranes were re-blotted with anti-Btk, 43-38 (Btk). (**e**) (Left) Effects of PI3K inhibitors on tyrosine phosphorylation of Btk. WT B cells were stimulated by BCR crosslinking (Anti-μ) in the absence or presence of 50 nM wortmannin (WN) or 25 μM Ly294002 (Ly). Btk was then immunoprecipitated and immunoblotted with 4G10 (p-Btk). Membranes were re-blotted with 43-38 (Btk). At the same time, cell lysates were examined for Akt phosphorylation by anti-phospho-Akt(S473) (p-Akt). Membranes were re-blotted with anti-Akt (Akt). (Right) Membrane fractions were prepared from WT and $PI3K^{-/-}$ B cells unstimulated or stimulated by BCR crosslinking (Anti-μ) in the absence or presence of 25 μM Ly294002 (Ly), and examined for tyrosine phoshorylation (p-Btk). Membranes were re-blotted with anti-Lyn (Lyn). Data in (**d**) and (**e**) are representative of three independent experiments with similar results. (**f,g**) BCR-induced activation of Btk. WT and $PI3K^{-/-}$ B cells on a BALB/c background were stimulated with or without 20 μg/ml of anti-IgM $F(ab)'_2$ (Anti-μ) at 37 °C for 3 min in the presence or absence of 10 μM Ly294002 (Ly). (**f**) Btk was immunoprecipitated and incubated with or without 100 μM ATP at 22 °C for 5 min followed by immunoblot analysis with 4G10. (**g**) Immunoprecipitates were incubated with acid-denatured enolase as an exogenous substrate in the presence of 100 μM ATP at 22 °C for 5 min. Btk activities are presented as the fold increase in the level of tyrosine phosphorylation of enolase. Data in (**f**) and (**g**) are representative of two independent experiments with similar results.

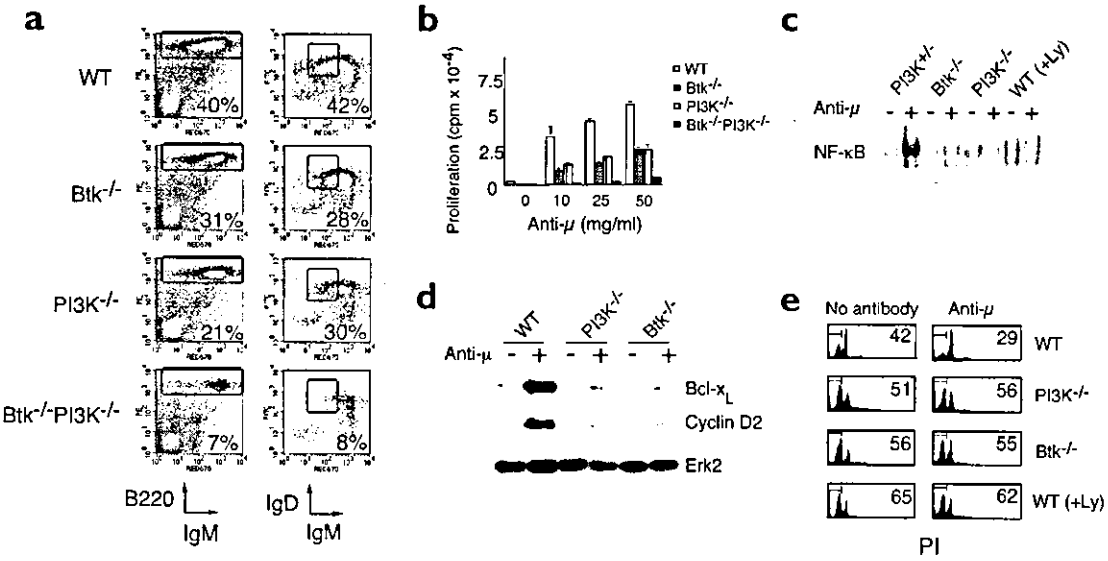

Figure 2. Phenotypes of PI3K and Btk double-deficient mice. (**a**) Splenocytes of indicated mice were stained with FITC-conjugated anti-IgD, PE-conjugated anti-B220 and biotinylated anti-IgM followed by Red670-conjugated streptavidin and examined by flow cytometry. IgM *versus* B220 profiles are shown on the left and IgM *versus* IgD profiles among B220$^+$ cells are shown on the right. Boxes in the left and right panels indicate total B cell and IgM^{lo}-IgD^{hi} circulating B cell fractions, respectively. (**b**) Proliferative responses of splenic B cells upon BCR stimulation *in vitro*. Proliferative responses are shown as [^{3}H]thymidine incorporation. Data are representative of two independent experiments with similar results. (**c**) NF-κB activation. PI3K$^{-/-}$ and Btk$^{-/-}$ B cells were stimulated with anti-μ in the absence or presence of Ly294002 (+Ly) for 4 h and nuclear extracts prepared. EMSA was carried out using ^{32}P-labeled NF-κB probe. (**d**) Induction of Bcl-x$_L$ and cyclin D2. Purified B cells of the indicated mice were stimulated with anti-μ for 16 h and evaluated for the expression of Bcl-x$_L$ and cyclin D2 by immunoblotting using specific antibodies. Membrane was re-blotted with anti-Erk2 (Erk2). (**e**) Apoptotic cell death in suspension culture. WT, PI3K$^{-/-}$ and Btk$^{-/-}$ B cells in the absence or presence of Ly294002 (+Ly) were incubated for 18 h and cell death was evaluated by DNA content analysis using propidium iodide. Numbers indicate the proportion of cells in the sub-G1 fraction (%) in cell cycle analysis. Data are representative of three independent experiments with similar results.

was severely blocked in the absence of PI3K (**Fig. 1c**). In contrast, BCR-mediated phosphorylation of Akt was unaffected in Btk$^{-/-}$ B cells (**Fig. 1c**), as shown previously[29]. Thus, BCR-mediated activation of Akt depends on PI3K, but not on Btk.

Activation of Btk is independent of PI3K

The phenotypic resemblance between PI3K$^{-/-}$ and Btk$^{-/-}$ mice in B cell developmental and activation defects suggests functional association between PI3K and Btk in BCR-mediated signal transduction[4,5]. If PI3K functions directly, and only, upstream of Btk, activation of Btk upon BCR stimulation would be expected to be impaired in PI3K$^{-/-}$ B cells. To this end, we examined the activation of Btk upon BCR stimulation (**Fig. 1d,e**).

First, purified B cells from PI3K$^{-/-}$ and WT mice were stimulated with a F(ab)'$_2$ fragment of anti-IgM and activation of immunoprecipitated Btk was evaluated by immunoblotting with the phosphotyrosine-specific mAb, 4G10. Contrary to our expectation, tyrosine phosphorylation of Btk induced by BCR crosslinking was unaffected in the absence of PI3K (**Fig. 1d**). Furthermore, addition of wortmannin had little effect on tyrosine phosphorylation of Btk in both PI3K$^{-/-}$ and WT B cells. Another PI3K inhibitor, Ly294002 also showed no effect on tyrosine phosphorylation of Btk (**Fig. 1e**, left). Both 50 nM wortmannin and 25 μM Ly294002, which inhibit all types of PI3Ks, did not block tyrosine phosphorylation of Btk, whereas these inhibitors completely block Akt activation in the same cells (**Fig. 1e**, left). Recruitment of phosphorylated Btk to the plasma membrane was also unaffected by inhibition of PI3K or by the lack of PI3K (**Fig. 1e**, right).

Next, we directly examined the kinase activity of Btk using an *in vitro* kinase assay system. BCR-induced activation of Btk activity, as examined by autophosphorylation of Btk, was unaffected in PI3K$^{-/-}$ B cells or by PI3K inhibitors (**Fig. 1f**). Likewise, Btk activation, as examined by phosphorylation of an exogenous substrate, enolase, was observed in the presence of Ly294002 (**Fig. 1g**). These results indicate that Btk can be activated in the absence of PI3K activity.

Phenotypes of PI3K$^{-/-}$Btk$^{-/-}$ double-deficient mice

To further examine if the activation of Btk can occur independent of PI3K in BCR signal transduction pathways, we used a genetic approach by comparing the phenotypes of single-deficient mice and PI3K$^{-/-}$Btk$^{-/-}$ double-deficient mice. If PI3K simply functions upstream of Btk by providing PIP_3 to the PH domain of Btk, the phenotype of double-deficient mice would be identical to that of PI3K or Btk single-deficient mice. On the other hand, if PI3K and Btk function independently in BCR signal transduction pathways, double-deficient mice should show a more severe phenotype. To this end, PI3K$^{-/-}$ and Btk$^{-/-}$ mice were crossed and analyzed. The number of mature (B220$^+$, IgM$^+$) splenic B cells in PI3K$^{-/-}$Btk$^{-/-}$ double-mutant mice was significantly ($P < 0.05$) less than that of each single-mutant counterpart (**Fig. 2a** and **Table 1**).

Table 1. Lymphocyte numbers in the spleen of Btk$^{-/-}$, PI3K$^{-/-}$ and PI3K$^{-/-}$Btk$^{-/-}$ mice

Genotype[a]	No. of B cells (× 10^6)	No. of IgM B cells (× 10^6)	No. of T cells (× 10^6)	B/T cell ratio
WT (n = 5)	28.3 ± 1.8	10.8 ± 1.0	28.7 ± 1.8	1.0 ± 0.1
Btk$^{-/-}$ (n = 7)	10.0 ± 2.4[b]	1.6 ± 1.5[e]	16.4 ± 2.0[h]	0.62 ± 0.17[j]
PI3K$^{-/-}$ (n = 5)	11.7 ± 4.8[b]	5.0 ± 3.4[e,f]	19.3 ± 5.8[h]	0.64 ± 0.28[j]
PI3K$^{-/-}$Btk$^{-/-}$ (n = 3)	6.2 ± 1.4[b,c,d]	1.0 ± 0.6[e,g]	22.5 ± 4.7	0.28 ± 0.06[h,k]

[a]Mice are on a mixed background between C57BL/6 and 129/Sv. Significance examined by Student-Newman-Keuls test: [b]$P < 0.01$ from WT; [c]$P < 0.05$ from Btk$^{-/-}$; [d]$P < 0.05$ from PI3K$^{-/-}$; [e]$P < 0.01$ from WT; [f]$P < 0.05$ from Btk$^{-/-}$; [g]$P < 0.05$ from PI3K$^{-/-}$; [h]$P < 0.01$ from WT; [i]$P < 0.05$ from WT; [j]$P < 0.01$ from WT; [k]$P < 0.05$ from Btk$^{-/-}$; [l]$P < 0.05$ from PI3K$^{-/-}$. Essentially the same results were obtained by statistical analysis using the Bonferroni correction method.

The number of circulating ($B220^+$, IgM^{low}, IgD^{high}) B cells among mature ($B220^+$, IgM^+) B cells in the spleen of $PI3K^{-/-}Btk^{-/-}$ double-deficient mice was also significantly ($P < 0.05$) lower than that in $PI3K^{-/-}$ mice, but was similar to that of $Btk^{-/-}$ mice (**Table 1**). When B/T cell ratios were compared, double-deficient mice show significantly ($P < 0.05$) lower B/T ratios than do single-deficient mice.

We next investigated the proliferative response of double-deficient B cells. Although BCR-induced proliferation of splenic B cells was impaired in $PI3K^{-/-}$ or $Btk^{-/-}$ mice, the response of double-deficient B cells was even lower than that of single-mutant B cells (**Fig. 2b**). These genetic data support the biochemical evidence that PI3K and Btk function independently in B cell signal transduction pathways.

Impaired induction of NF-κB and Bcl-x_L

BCR stimulation activates the NF-κB pathway and both Akt and Btk are involved in NF-κB activation in B cells[30-33]. We thus investigated BCR-mediated activation of NF-κB in $PI3K^{-/-}$ and $Btk^{-/-}$ B cells. In normal B cells, the activity of nuclear NF-κB complexes containing p50 and c-Rel was increased upon BCR stimulation as revealed by electrophoretic mobility shift assay (EMSA) analysis (**Fig. 2c** and data not shown). On the contrary, activation of NF-κB was reduced in $PI3K^{-/-}$ B cells and in Ly294002-treated WT B cells, indicating that BCR-dependent NF-κB activation involves the PI3K pathway. BCR-mediated activation of NF-κB was also blocked in $Btk^{-/-}$ B cells (**Fig. 2c**), as previously reported[31,32]. Thus, BCR-dependent activation of NF-κB requires both PI3K and Btk.

NF-κB is known to have a role in the induction of Bcl-x_L and cyclin D2 upon BCR stimulation[34,35]. Bcl-x_L induction after BCR stimulation was impaired in $PI3K^{-/-}$ and $Btk^{-/-}$ B cells (**Fig. 2d**). Furthermore, induction of cyclin D2, indicative of cell cycle progression, was blocked in both $PI3K^{-/-}$ and $Btk^{-/-}$ B cells (**Fig. 2d**), consistent with the observed BCR-induced proliferative responses (**Fig. 2b**). These results suggest that NF-κB-Bcl-x_L and NF-κB-cyclin D2 pathways are common downstream targets of PI3K and Btk in BCR-mediated signal transduction.

As BCR-dependent induction of Bcl-x_L was impaired in both $PI3K^{-/-}$ and $Btk^{-/-}$ mice, one prediction was that these mutant B cells would be more susceptible to apoptosis than WT B cells. We thus examined apoptotic cell death in suspension culture of $PI3K^{-/-}$ and $Btk^{-/-}$ B cells with or without BCR stimulation. Apoptotic death after an 18-h incubation was evaluated by the proportion of cells in the sub-G1 fraction in cell cycle analysis using propidium iodide staining (**Fig. 2e**). We found that 40% of splenic B cells showed apoptosis after 18 h cultivation *in vitro* without stimulation, and such spontaneous cell death in suspension culture was enhanced in the absence of PI3K or Btk (**Fig. 2e**). Although BCR stimulation with anti-IgM $F(ab)'_2$ fragment results in a partial rescue of WT B cells from apoptosis, BCR stimulation was unable to rescue $PI3K^{-/-}$ and $Btk^{-/-}$ B cells (**Fig. 2e**). These results indicate both $PI3K^{-/-}$ and $Btk^{-/-}$ B cells have an increased sensitivity to cell death, possibly because of the failure of BCR-mediated Bcl-x_L induction.

Forced expression of Bcl-x_L in $PI3K^{-/-}$ B cells

As shown above, the inability to induce Bcl-x_L may lead to the low B cell numbers as well as the low proliferative response of $PI3K^{-/-}$ and $Btk^{-/-}$ B cells, and may explain the phenotypic resemblance between $PI3K^{-/-}$ and $Btk^{-/-}$ mice. It has been shown that forced expression of Bcl-x_L in *Xid* mice restores B cell development and proliferative responses[36]. We thus examined the effect of overexpression of Bcl-x_L in $PI3K^{-/-}$ B cells by generating Bcl-x_L transgenic $PI3K^{-/-}$ mice. Equivalent numbers of mature B cells and circulating B cells were found in Bcl-x_L transgenic $PI3K^{-/-}$ mice and WT mice (**Fig. 3a** and **Table 2**). When B/T cell ratios were compared, it was also apparent that the transgenic expression of Bcl-x_L in $PI3K^{-/-}$ mice restored the relative lymphocyte composition to that found in WT mice.

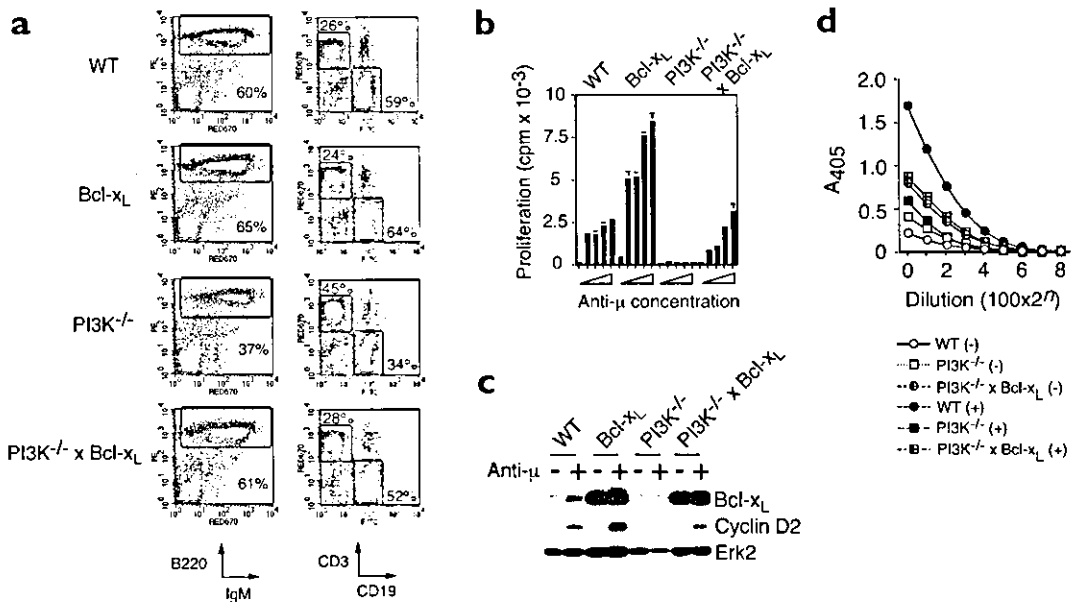

Figure 3. Restoration of B cell numbers and proliferative response of $PI3K^{-/-}$ mice by transgenic expression of Bcl-x_L. (**a**) Splenocytes of indicated mice were stained with a combination of PE-conjugated anti-B220 and biotinylated anti-IgM followed by Red670-conjugated streptavidin, or FITC-conjugated anti-CD19 and biotinylated anti-CD3 followed by Red670-conjugated streptavidin, and examined by flow cytometry. IgM *versus* B220 profiles are shown on the left and CD19 *versus* CD3 profiles to examine the ratio of B and T cells are shown on the right. Boxes in the left panels indicate B cell fractions. Top and bottom boxes in the right panels indicate T and B cell fractions, respectively. (**b**) Purified B cells of the indicated mice were examined for their proliferative responses following BCR stimulation as in **Fig. 2b**. Concentrations of anti-μ were 0, 5, 10, 25 and 50 μg/ml from left to right for each group. (**c**) Induction of cyclin D2 by forced expression of Bcl-x_L. Purified B cells of the indicated mice were stimulated with anti-BCR for 18 h and examined for the expression of Bcl-x_L and cyclin D2. Note the constitutive expression of Bcl-x_L in Bcl-x_L transgenic B cells. Membrane was re-blotted with anti-Erk2 (Erk2). (**d**) T lymphocyte-independent antibody production of indicated mice using DNP-Ficoll was examined as described[3]. The immune sera (+) were analyzed at day 7 for DNP specific total immunoglobulin by ELISA and titers were shown as absorbance at 405-nm wavelength (A_{405}). Preimmune sera (-) were used as controls. Data are representative of two independent experiments with similar results.

Finally, we examined the functions of B cells in Bcl-x_L transgenic PI3K$^{-/-}$ mice. PI3K$^{-/-}$ B cells were incapable of proliferating in response to BCR stimulation[4,5], but the proliferative response of Bcl-x_L transgenic PI3K$^{-/-}$ B cells was similar to that of WT B cells (**Fig. 3b**). Consistent with these results, transgenic expression of Bcl-x_L increased the expression of cyclin D2 in PI3K$^{-/-}$ B cells (**Fig. 3c**). These results indicate that the lack of Bcl-x_L induction is a common defect in PI3K$^{-/-}$ and Btk$^{-/-}$ B cells leading to the similar phenotypes seen in PI3K$^{-/-}$ and Btk$^{-/-}$ mice. On the other hand, T cell-independent antibody production in response to dinitrophenyl (DNP)-Ficoll, which is impaired in PI3K$^{-/-}$ mice[4], was not restored by introduction of the Bcl-x_L transgene (**Fig. 3d**), indicating that the expression of Bcl-x_L alone is insufficient for the restoration of some of the functional defects observed in PI3K$^{-/-}$ mice.

Table 2. Restoration of splenic B cell numbers in PI3K$^{-/-}$ mice by Bcl-x_L expression

Genotype[a]	No. of B cells ($\times 10^6$)	No. of IgM^{low} B cells ($\times 10^6$)	No. of T cells ($\times 10^6$)	B/T cell ratio
WT (n = 6)	34.2 ± 9.1	17.3 ± 5.3	27.1 ± 9.9	1.32 ± 0.32
Bcl-x_L tg (n = 4)	56.4 ± 16.7[b]	28.7 ± 9.3[e]	29.5 ± 9.2	1.99 ± 0.44
PI3K$^{-/-}$ (n = 7)	21.0 ± 6.7[b,c]	6.3 ± 2.2[f,g]	35.6 ± 3.2	0.60 ± 0.15[i,j]
PI3K$^{-/-}$ × Bcl-x_L tg (n = 7)	48.2 ± 10.0[d]	14.3 ± 4.6[g,h]	36.1 ± 11.2	1.42 ± 0.43[k]

[a]Mice are on a C57BL/6 background. Significance examined by Student-Newman-Keuls test: [b]$P < 0.05$ from WT; [c]$P < 0.01$ from Bcl-x_L tg; [d]$P < 0.01$ from PI3K$^{-/-}$; [e]$P < 0.05$ from WT; [f]$P < 0.01$ from WT; [g]$P < 0.01$ from Bcl-x_L tg; [h]$P < 0.05$ from PI3K$^{-/-}$; [i]$P < 0.01$ from WT; [j]$P < 0.01$ from Bcl-x_L tg; [k]$P < 0.01$ from PI3K$^{-/-}$.

Discussion

Contrary to the current model, in which PI3K acts directly upstream of Btk, tyrosine phosphorylation and subsequent activation of kinase activity of Btk was unaffected by the lack of PI3K or by PI3K inhibitors. There have been a few hints previously that this might be the case. BCR-induced Btk activation is blocked only marginally by wortmannin at 50 nM in the B cell line J558Lμm3[37]. Overexpression of the p110 catalytic subunit of PI3K in fibroblasts as well as in the B cell line A20B results in tyrosine phosphorylation of Btk. In this case as well, tyrosine phosphorylation of Btk is only modestly blocked by wortmannin, even at 100 nM, implying the presence of a PI3K-independent pathway for Btk activation[21]. A recent study further shows that tyrosine phosphorylation of Btk is unaffected in B cells deficient for p110δ, the most abundantly expressed catalytic isoform of class I_A PI3K[38]. Phenotypes of PI3K$^{-/-}$Btk$^{-/-}$ double-deficient mice were consistent with these observations. We repeatedly observed higher amounts of tyrosine phosphorylation of Btk in PI3K$^{-/-}$ B cells than in WT B cells. Likewise, PI3K$^{-/-}$ B cells showed higher kinase activity than WT B cells. The reason for the hyperactivation of Btk in PI3K$^{-/-}$ B cells is unknown at present.

The fact that a point mutation within the PH domain of Btk (in which an arginine residue critical for the binding to PIP_3 is replaced by cysteine) leads to *Xid* also supports the current model[12,15,16]. In the DT40 chicken B cell system, targeted disruption of Btk results in impaired activation of phospholipase C-γ2, which is restored by transfection of WT Btk, but not Btk with the *Xid* mutation[39]. In our hands, however, the mutant Btk protein produced from the gene carrying the *Xid* mutation was unstable and degraded rapidly when expressed in cells by gene transfer (data not shown). It is possible that the defect caused by the *Xid* mutation is not due to the inability to bind PIP_3, but to the degradation of the mutant protein. It was theoretically possible that Btk functions upstream of PI3K, but the fact that PI3K was activated in the absence of Btk excluded this possibility.

Recruitment of phosphorylated Btk to the plasma membrane was also unaffected by PI3K inhibitors or in PI3K$^{-/-}$ B cells. Recent studies have raised the possibility that Btk is recruited to the plasma membrane through a mechanism independent of PIP_3 generation. Identification of an adapter protein, BLNK (also known as SLP65), and its involvement in Btk activation support this alternative possibility[17,18]. In fact, BLNK is phosphorylated by Syk and provides Btk with docking sites to bring them into close proximity. Btk is then activated by tyrosine phosphorylation after binding to BLNK upon BCR stimulation. At the same time, BLNK is recruited to the plasma membrane upon BCR stimulation by binding to the BCR complex, which leads to the recruitment of Btk to the plasma membrane[40]. Involvement of such molecular mechanisms of recruiting Btk to the plasma membrane should be evaluated for a better understanding of the role of Btk in BCR signaling. Although PI3K and Btk likely function independently in B cell signal transduction pathways and have unique roles in proximal BCR signaling, we do not exclude the possibility that the interaction between PIP_3 and the PH domain is more critical for the activation of Btk, and possibly other Tec family kinases, in other cell types with different receptor systems.

BCR-mediated activation of Akt was completely blocked in the absence of PI3K. Activation of Akt is a multi-step reaction involving the generation of PIP_2 and PIP_3, which recruit Akt and PDK1, respectively, to the plasma membrane[22,23]. Although the role of Btk in Akt activation is controversial in the chicken DT40 B cell system[22,41], Akt activation, as revealed by phosphorylation of two critical residues in primary Btk$^{-/-}$ B cells, was unaffected. Thus, activation of Akt is dependent on class I_A PI3K containing p85α, but is independent of Btk in mouse primary B cells. Akt binds and activates IKK to induce degradation of IκB and activation of NF-κB[42]. Btk is also required for the activation of NF-κB in B cells[31,32]. Because activation of Akt does not depend on Btk in mouse B cells, it is likely that both Btk-dependent and Akt-dependent distinct pathways are required for activating NF-κB in B cells.

Induction of both Bcl-x_L and cyclin D2 involves NF-κB–mediated transcriptional activation. For example, overexpression of dominant-negative NF-κB inhibited CD40-mediated Bcl-x_L induction[43] and transgenic mice expressing a constitutively active, membrane-anchored Akt showed elevated activation of NF-κB and Bcl-x_L[44]. Bcl-x_L is a major anti-apoptotic protein that is induced upon BCR stimulation[35]. Consistent with these observations, PI3K$^{-/-}$ B cells and Btk$^{-/-}$ B cells showed increased apoptosis compared with WT B cells. Previously, we observed little significant difference in viability between PI3K$^{+/-}$ and PI3K$^{-/-}$ B cells upon BCR stimulation, as measured by annexin V staining[4]. However, we noted that annexin V staining is higher on B cells than on other cell types[45] and is not a sensitive method for measuring apoptotic B cells. As shown here, propidium iodide staining seems to be a better method to evaluate apoptosis in B cells. The lack of Bcl-x_L as well as cyclin D2 induction may be the cause of the phenotypic similarity between PI3K$^{-/-}$ and Btk$^{-/-}$ mice. In fact, forced expression of Bcl-x_L as a transgene restored B cell development and proliferative responses similar to what has been observed in *Xid* B cells[36]. These results also support our conclusion that the NF-κB-Bcl-x_L pathway is a

common target of PI3K- and Btk-dependent distinct signaling pathways in B cell activation. As observed in *Xid* mice, however, T cell-independent antibody production was not restored by introduction of the Bcl-x_L transgene, indicating that the expression of Bcl-x_L alone is insufficient for the restoration of some of the functional defects caused by the lack of Btk and PI3K.

Biochemical and genetic approaches revealed that class I_A PI3K and Btk constitute functionally distinct signaling pathways proximal to the membrane, but share a common downstream target, the NF-κB-Bcl-x_L pathway, in BCR-mediated signal transduction. The lack of activation of the NF-κB-Bcl-x_L pathway likely leads to the similarity of phenotypes in $PI3K^{-/-}$ and $Btk^{-/-}$ mice. The mechanisms that coordinate the PI3K-Akt and Btk pathways in the activation of NF-κB remain to be determined.

Methods

Mice. PI3K-deficient mice[34] were backcrossed to C57BL/6 or BALB/c mice for more than seven generations before intercrossing heterozygous mice[46,47]. Mice on a C57BL/6 background were used unless otherwise mentioned. $Btk^{-/-}$ mice on a (C57BL/6 × 129/Sv) mixed background were purchased from The Jackson Laboratory (Bar Harbor, ME). Because Btk is encoded on the X chromosome, Btk-deficient female and male mice have the $Btk^{-/-}$ and $Btk^{-/y}$ genotypes, respectively. Hence, we designate Btk-deficient mice as $Btk^{-/-}$ mice. $PI3K^{-/-}Btk^{-/-}$ double-deficient mice were generated by crossing $PI3K^{-/-}$ and $Btk^{-/-}$ mice to generate F2 mice carrying the $PI3K^{-/-}Btk^{-/-}$ genotype. Bcl-x_L transgenic mouse line #87 on a C57BL/6 background has been described[35,48]. In this transgenic mouse line, human Bcl-x_L protein is driven by the SV40 promoter and Eμ enhancer and is abundantly expressed in B cells. Bcl-x_L transgenic and $PI3K^{-/-}$ mice were crossed to generate $PI3K^{-/-}$ mice expressing the Bcl-x_L transgene in $PI3K^{-/-}$ B cells. All mice were maintained at Taconic (Germantown, NY) or in our animal facility under specific pathogen-free conditions. All experiments were performed in accordance with our Institutional Guidelines.

Reagents. Antibodies to cyclin D2, Erk2, Btk and Lyn were purchased from Santa Cruz Biotechnology (Santa Cruz, CA). Anti–Bcl-x_L was obtained from Transduction Laboratories (Lexington, KY). A mAb to Btk, 43-3B[49], was a generous gift from S. Tsukada (Osaka University, Osaka, Japan). Anti-$p85^{pan}$ was purchased from Upstate Biotechnology (Lake Placid, NY). Anti-Akt, anti-phospho-Akt(S473) and anti-phospho-Akt(T308) were from Cell Signaling Technology (Beverly, MA). Specific antisera for p85β and p55γ have been described[7]. Anti-phosphotyrosine antibody (4G10) was a gift from T. Roberts (DFCI, Boston, MA). PI3K-specific inhibitors, wortmannin and Ly294002, were purchased from Calbiochem (La Jolla, CA).

Flow cytometric analysis. Fluorescein isothiocyanate (FITC)-conjugated anti-mouse IgM, FITC-conjugated anti-mouse IgD, FITC-conjugated anti-CD19, phycoerythrin (PE)-conjugated anti-B220, biotinylated anti-mouse IgM and biotinylated anti-CD3 were purchased from PharMingen (San Diego, CA). Binding of biotinylated mAbs was detected with streptavidin-Red670 (GIBCO BRL, Grand Island, NY). One to two million cells were stained with designated antibodies in PBS with 2% fetal calf serum (FCS) and subjected to analysis on a FACScan using the CELLQuest program (Becton Dickinson, San Jose, CA).

Cell stimulation and immunoblotting. B cells were purified from total splenocytes using anti-B220-coated magnetic beads and AutoMACS (Miltenyi Biotech, Sunnyvale, CA). Purity of the cells was >95%. We resuspended 2–7 × 10^7 purified B cells in 1 ml of culture medium and preincubated them for 15 min at 37 °C with or without inhibitors. Cells were then stimulated with $F(ab')_2$ fragment of goat polyclonal antibody to mouse IgM (anti-IgM $F(ab')_2$, 40 μg/ml; Jackson ImmunoResearch, West Grove, PA) and incubated at 37 °C for the indicated time. Cells were collected, lysed in a lysis buffer solution (1% NP-40, 50 mM Tris, pH 7.4, 150 mM NaCl, 2 mM EDTA, 10 μg/ml leupeptin, 10 μg/ml aprotinin, 1 μg/ml pepstatin A, 50 μM phenylmethylsulfonyl fluoride (PMSF), 1 mM Na-vanadate) and immunoprecipitated with the indicated antibodies or directly applied to SDS-PAGE and transferred to polyvinyldifluoride (PVDF) membranes. Reactive proteins were visualized with ECL Chemiluminescent substrates (NEN, Boston, MA). To examine phosphorylation of Btk in the membrane fraction, cells were lysed with 300 μl of hypotonic buffer solution (10 mM HEPES, pH 7.9, 10 mM NaF, 1.5 mM $MgCl_2$, 10 mM KCl, 1 mM benzamidine, 2 mM EGTA, 2 mM DTT, 1 mM vanadate, 1 mM PMSF, 1% aprotinin) using a Dounce homogenizer. Lysates were centrifuged at 10,000*g* for 30 s, and the supernatant was further centrifuged at 100,000*g* for 30 min to obtain S100 (supernatant) and P100 (pellet). P100 was subjected to immunoblot analysis with 4G10 and anti-Lyn.

PI3K activity. Activation-induced PI3K activity in B cells was estimated as PI3K activity among tyrosine phosphorylated proteins[1]. After BCR stimulation, cell lysates were immunoprecipitated with 4G10 and subjected to *in vitro* PI3K assay. Briefly, immunoprecipitate was incubated with phosphatidylinositol and γ-[^{32}P]ATP for 15 min at room temperature, and the chloroform extract was separated by thin-layer chromatography.

Btk activity. Splenic B cells (6 × 10^7) were stimulated with or without 20 μg/ml of anti-IgM $F(ab')_2$ at 37 °C for 3 min in the presence or absence of PI3K inhibitors, and lysed in an extraction buffer solution (20 mM Tris, pH 7.4, 2 mM EGTA, 12.5 mM β-glycerophosphate, 10 μg/ml leupeptin, 10 μg/ml pepstatin A, 2 mM DTT, 1 mM PMSF, 1 mM vanadate, 1% aprotinin) containing 0.2% Triton X-100. For immunoprecipitation, 15 μg of an anti-Btk was coupled to protein A Sepharose at 4 °C overnight. The beads were washed once with extraction buffer solution and incubated with precleared total cell lysates for 1 h at 4 °C. Subsequently, the beads were washed twice with extraction buffer solution containing 1% Triton X-100 and once with extraction buffer solution alone, followed by incubation with or without 100 μM ATP at 22 °C for 5 min. Samples were subjected to immunoblot analysis with 4G10. Or, immunocomplex was incubated with 5 μg of acid-denatured enolase as an exogenous substrate in the presence of 100 μM ATP at 22 °C for 5 min.

EMSA. Preparation of nuclear extract and EMSA were carried out as described[31,32]. Briefly, 10 μg nuclear extract was incubated with 20 fmol ^{32}P-labeled NF-κB probe (Santa Cruz). The DNA-protein complexes were resolved on a native 5% polyacrylamide gel, dried and exposed to an x-ray film for autoradiography. Identity of the band was confirmed by anti-p50 (Santa Cruz)-induced supershift (data not shown).

Cell proliferation and cell cycle analysis. Purified B cells (0.5 to 1 × 10^5/well) were treated with the indicated concentrations of anti-IgM $F(ab')_2$ in culture medium containing 2 ng/ml rIL-4 (Pepro Tech $EC_{1.0}$, London, England) in 96-well plates for 72 h. [^{3}H]Thymidine (3.7 × 10^4 Bq (1 μCi)/well) was added to the cultures during the last 16 h and uptake of radioactivity was measured by liquid scintillation counter. For cell cycle analysis, splenic B cells were activated with anti-IgM $F(ab')_2$ *in vitro* for 18 h, fixed with 70% ethanol and treated with RNaseA (1 mg/ml). Fixed cells were stained with 50 μg/ml propidium iodide for 3 h at room temperature and analyzed on a FACScan (Beckton Dickinson).

Antibody production. Mice were pre-bled and immunized intraperitoneally with 100 μg DNP-keyhole lympet hemocyanin (KLH; LSL, Tokyo, Japan) in a 1:1 emulsion with Freund's complete adjuvant (Sigma), or 10 μg DNP-Ficoll in PBS at day 0. The serum was analyzed at day 7 for DNP specific total immunoglobulin by ELISA.

Acknowledgments

We thank N. Watanabe and M. Handa for help in some experiments; C. Maki for technical assistance; A. Sakurai, M. Motouchi and K. Furuichi for animal care; and Y. Fukui, T. Kurosaki and L.K. Clayton for suggestions and critical reading of the manuscript. This work was supported in part by a Grant-in-Aid for Creative Scientific Research (13GS0015), a Grant-in-Aid for Scientific Research (A) (13307012), (B) (14370116) and (C) (13670322), and a Grant-in-Aid for Scientific Research on Priority Areas (13037028) from the Japan Society for the Promotion of Science, a National Grant-in-Aid for the Establishment of a High-Tech Research Center in a private University, a grant for the Promotion of the Advancement of Education and Research in Graduate Schools, and a Scientific Frontier Research Grant from the Ministry of Education, Culture, Sports, Science and Technology, Japan.

Competing interests statement

The authors declare that they have no competing financial interests.

Received 1 May 2002; accepted 2 January 2003.

1. Fruman, D.A., Meyers, R.E. & Cantley, L.C. Phosphoinositide kinases. *Annu. Rev. Biochem.* **67**, 481–507 (1998).
2. Katso, R. *et al.* Functions of phosphoinositide 3-kinases: implications for development, immunity, homeostasis, and cancer. *Annu. Rev. Cell Dev. Biol.* **17**, 615–675 (2001).
3. Terauchi, Y. *et al.* Increased insulin sensitivity and hypoglycaemia in mice lacking the p85α subunit of phosphoinositide 3-kinase. *Nat. Genet.* **21**, 230–235 (1999).
4. Suzuki, H. *et al.* *Xid*-like immunodeficiency in mice with disruption of the p85α subunit of phosphoinositide 3-kinase. *Science* **283**, 390–392 (1999).
5. Fruman, D.A. *et al.* Impaired B cell development and proliferation in absence of phosphoinositide 3-kinase p85α. *Science* **283**, 393–397 (1999).
6. Fruman, D.A., Cantley, L.C. & Carpenter, C.L. Structural organization and alternative splicing of the murine phosphoinositide 3-kinase p85α gene. *Genomics* **37**, 113–121 (1996).
7. Inukai, K. *et al.* p85α gene generates three isoforms of regulatory subunit for phosphatidylinositol 3-kinase (PI 3-Kinase), p50α, p55α, and p85α, with different PI 3-kinase activity elevating responses to insulin. *J. Biol. Chem.* **272**, 7873–7882 (1997).
8. Campbell, K.S. Signal transduction from the B cell antigen-receptor. *Curr. Opin. Immunol.* **11**, 256–264 (1999).
9. Kurosaki, T. Genetic analysis of B cell antigen receptor signaling. *Annu. Rev. Immunol.* **17**, 555–592 (1999).
10. Marshall, A.J., Niiro, H., Yun, T.J. & Clark, E.A. Regulation of B-cell activation and differentiation by the phosphatidylinositol 3-kinase and phospholipase Cγ pathway. *Immunol. Rev.* **176**, 30–46 (2000).
11. Tedder, T.F., Sato, S., Poe, J.C. & Fujimoto, M. CD19 and CD22 regulate a B lymphocyte signal transduction pathway that contributes to autoimmunity. *Keio J. Med.* **49**, 1–13 (2000).
12. Tsukada, S., Baba, Y. & Watanabe, D. Btk and BLNK in B cell development. *Adv. Immunol.* **77**, 123–162 (2001).
13. Salim, K. *et al.* Distinct specificity in the recognition of phosphoinositides by the pleckstrin homology domains of dynamin and Bruton's tyrosine kinase. *EMBO J.* **15**, 6241–6250 (1996).
14. Fukuda, M., Kojima, T., Kabayama, H. & Mikoshiba, K. Mutation of the pleckstrin homology domain of Bruton's tyrosine kinase in immunodeficiency impaired inositol 1,3,4,5-tetrakisphosphate binding capacity. *J. Biol. Chem.* **271**, 30303–30306 (1996).
15. Satterthwaite, A.B., Li, Z. & Witte, O.N. Btk function in B cell development and response. *Semin. Immunol.* **10**, 309–316 (1998).
16. Tarakhovsky, A. *Xid* and *Xid*-like immunodeficiencies from a signaling point of view. *Curr. Opin.*

Immunol. **3**, 319–323 (1997).
17. Fu, C., Turck, C.W., Kurosaki, T. & Chan, A.C. BLNK: a central linker protein in B cell activation. *Immunity* **9**, 93–103 (1998).
18. Kurosaki, T. & Tsukada, S. BLNK: connecting Syk and Btk to calcium signals. *Immunity* **12**, 1–5 (2000).
19. Varnai, P., Rother, K.I. & Balla, T. Phosphatidylinositol 3-kinase-dependent membrane association of the Bruton's tyrosine kinase pleckstrin homology domain visualized in single living cells. *J. Biol. Chem.* **274**, 10983–10989 (1999).
20. Nore, B.F. *et al.* Redistribution of Bruton's tyrosine kinase by activation of phosphatidylinositol 3-kinase and Rho-family GTPases. *Eur. J. Immunol.* **30**, 145–154 (2000).
21. Scharenberg, A.M. *et al.* Phosphatidylinositol-3,4,5-trisphosphate (PtdIns-3,4,5-P_3)/Tec kinase-dependent calcium signaling pathway: a target for SHIP-mediated inhibitory signals. *EMBO J.* **17**, 1961–1972 (1998).
22. Gold, M.R. *et al.* The B cell antigen receptor activates the Akt (protein kinase B)/glycogen synthase kinase-3 signaling pathway via phosphatidylinositol 3-kinase. *J. Immunol.* **163**, 1894–1905 (1999).
23. Coffer, P.J., Jin, J. & Woodgett, J.R. Protein kinase B (c-Akt): a multifunctional mediator of phosphatidylinositol 3-kinase activation. *Biochem. J.* **335**, 1–13 (1998).
24. Datta, S.R., Brunet, A. & Greenberg, M.E. Cellular survival: a play in three Akts. *Genes. Dev.* **13**, 2905–2927 (1999).
25. Hemmings, B.A. Akt signaling: linking membrane events to life and death decisions. *Science* **275**, 628–630 (1997).
26. Franke, T.F., Kaplan, D.R. & Cantley, L.C. PI3K: downstream AKTion blocks apoptosis. *Cell* **88**, 435–437 (1997).
27. Burgering, B.M. & Coffer, P.J. Protein kinase B (c-Akt) in phosphatidylinositol-3-OH kinase signal transduction. *Nature* **376**, 599–602 (1995).
28. Brozinick, J.T. Jr. & Birnbaum, M.J. Insulin, but not contraction, activates Akt/PKB in isolated rat skeletal muscle. *J. Biol. Chem.* **273**, 14679–14682 (1998).
29. Forssell, J., Nilsson, A. & Sideras, P. Reduced formation of phosphatidic acid upon B-cell receptor triggering of mouse B-lymphocytes lacking Bruton's tyrosine kinase. *Scand. J. Immunol.* **52**, 30–38 (2000).
30. Kane, L.P., Shapiro, V.S., Stokoe, D. & Weiss, A. Induction of NF-κB by the Akt/PKB kinase. *Curr. Biol.* **9**, 601–604 (1999).
31. Bajpai, U.D., Zhang, K., Teutsch, M., Sen, R. & Wortis, H.H. Bruton's tyrosine kinase links the B cell receptor to nuclear factor κB activation. *J. Exp. Med.* **191**, 1735–1744 (2000).
32. Petro, J.B., Rahman, S.M.J., Ballard, D.W. & Khan, W.N. Bruton's tyrosine kinase is required for activation of IκB kinase and nuclear factor κB in response to B cell receptor engagement. *J. Exp. Med.* **191**, 1745–1754 (2000).
33. Miyamoto, S., Schmitt, M.J. & Verma, I.M. Qualitative changes in the subunit composition of κ B-binding complexes during murine B-cell differentiation. *Proc. Natl. Acad. Sci. USA* **91**, 5056–5060 (1994).
34. Solvason, N. *et al.* Induction of cell cycle regulatory proteins in anti-immunoglobulin-stimulated mature B lymphocytes. *J. Exp. Med.* **184**, 407–417 (1996).
35. Anderson, J.S., Teutsch, M., Dong, Z. & Wortis, H.H. An essential role for Bruton's tyrosine kinase in the regulation of B-cell apoptosis. *Proc. Natl. Acad. Sci. USA* **93**, 10966–10971 (1996).
36. Solvason, N. *et al.* Transgene expression of bcl-xL permits anti-immunoglobulin (Ig)-induced proliferation in *xid* B cells. *J. Exp. Med.* **187**, 1081–1091 (1998).
37. Buhl, A.M. & Cambier, J.C. Phosphorylation of CD19 Y484 and Y515, and linked activation of phosphatidylinositol 3-kinase, are required for B cell antigen receptor-mediated activation of Bruton's tyrosine kinase. *J. Immunol.* **162**, 4438–4446 (1999).
38. Jou, S.T. *et al.* Essential, nonredundant role for the phosphoinositide 3-kinase p110δ in signaling by the B-cell receptor complex. *Mol. Cell. Biol.* **22**, 8580–8591 (2002).
39. Takata, M. & Kurosaki, T. A role for Bruton's tyrosine kinase in B cell antigen receptor-mediated activation of phospholipase C-γ2. *J. Exp. Med.* **184**, 31–40 (1996).
40. Engels, N., Wollscheid, B. & Wienands, J. Association of SLP-65/BLNK with the B cell antigen receptor through a non-ITAM tyrosine of Ig-α. *Eur. J. Immunol.* **31**, 2126–2134 (2001).
41. Craxton, A., Jiang, A., Kurosaki, T. & Clark, E.A. Syk and Bruton's tyrosine kinase are required for B cell antigen receptor-mediated activation of the kinase Akt. *J. Biol. Chem.* **274**, 30644–30650 (1999).
42. Romashkova, J.A. & Makarov, S.S. NF-κB is a target of AKT in anti-apoptotic PDGF signalling. *Nature* **401**, 86–90 (1999).
43. Lee, H.H., Dadgostar, H., Cheng, Q., Shu, J. & Cheng, G. NF-κB-mediated up-regulation of Bcl-x and Bfl-1/A1 is required for CD40 survival signaling in B lymphocytes. *Proc. Natl. Acad. Sci. USA* **96**, 9136–9141 (1999).
44. Jones, R.G. *et al.* Protein kinase B regulates T lymphocyte survival, nuclear factor κB activation, and Bcl-X(L) levels *in vivo*. *J. Exp. Med.* **191**, 1721–1734 (2000).
45. Dillon, S.R., Mancini, M., Rosen, A. & Schlissel, M.S. Annexin V binds to viable B cells and colocalizes with a marker of lipid rafts upon B cell receptor activation. *J. Immunol.* **164**, 1322–1332 (2000).
46. Fukao, T. *et al.* Selective loss of gastrointestinal mast cells and impaired immunity in PI3K-deficient mice. *Nat. Immunol.* **3**, 295–304 (2002).
47. Fukao, T. *et al.* PI3K-mediated negative feedback regulation of IL-12 production in dendritic cells. *Nat. Immunol.* **3**, 875–881 (2002).
48. Grillot, D.A.M. *et al.* Bcl-x exhibits regulated expression during B cell development and activation and modulates lymphocyte survival in transgenic mice. *J. Exp. Med.* **183**, 381–391 (1996).
49. Baba, Y. *et al.* Involvement of Wiskott-Aldrich syndrome protein in B-cell cytoplasmic tyrosine kinase pathway. *Blood* **93**, 2003–2012 (1999).

nature immunology

AID mutant analyses indicate requirement for class-switch-specific cofactors

Van-Thanh Ta[4], Hitoshi Nagaoka[4], Nadia Catalan[1], Anne Durandy[1], Alain Fischer[1], Kohsuke Imai[1,3], Shigeaki Nonoyama[2,3], Junko Tashiro[4], Masaya Ikegawa[4], Satomi Ito[4], Kazuo Kinoshita[4], Masamichi Muramatsu[4] & Tasuku Honjo[4]

Activation-induced cytidine deaminase (AID) is the essential and sole B cell–specific factor required for class-switch recombination (CSR) and somatic hypermutation (SHM). However, it is not known how AID differentially regulates these two independent events. Involvement of several cofactors interacting with AID has been indicated by scattered distribution of loss-of-function point mutations and evolutionary conservation of the entire 198-amino-acid protein. Here, we report that human AID mutant proteins with insertions, replacements or truncations in the C-terminal region retained strong SHM activity but almost completely lost CSR activity. These results indicate that AID requires interaction with a cofactor(s) specific to CSR.

Antigen stimulation of mature immunoglobulin M (IgM)-positive B lymphocytes induces two genetic events in their immunoglobulin gene loci; these events are essential for efficient antigen elimination. Class-switch recombination (CSR) replaces the heavy chain constant region (C_H) from C_μ to other C_H regions to diversify the effector function of the immunoglobulin. CSR takes place between switch (S) regions located 5′ to each C_H gene except for C_δ, resulting in juxtaposition of a given rearranged heavy chain variable region (V_H) gene to a new C_H gene and looping-out deletion of the intervening DNA segment[1,2]. The S region consists of G-rich repetitive sequences with abundant palindromes. The efficiency of antigen elimination is also augmented by affinity maturation, which is accomplished by excessive point mutations in the V-region gene, coupled with selection of high-affinity antibody-producing cells by limited amounts of antigen. Point mutations are introduced by two types of molecular mechanisms: non-templated SHM, and gene conversion, which takes place in chickens and rabbits, with pseudogenes serving as template[3].

AID is essential for all three genetic events: CSR, SHM and gene conversion[4–10]. AID shows homology with apolipoprotein B mRNA-editing catalytic subunit 1 (APOBEC-1), an RNA-editing enzyme of mRNA precursor apolipoprotein B 100, encoding low-density lipoprotein, and the two genes are located near each other on mouse and human chromosomes[11]. Such evolutionary conservation indicates that AID may be an RNA-editing enzyme for an mRNA precursor(s) encoding endonucleases that cleave the S- or V-region DNA. This model is supported by the finding that *de novo* protein synthesis is required for AID activity. As the mRNA edited by AID must be translated to exert the function of AID, de novo protein synthesis is obligatory[12]. In contrast, AID expression in *Escherichia coli* was shown to increase mutations, indicating that AID may directly act on DNA and convert C to U, followed by base excision repair to introduce DNA cleavage[13,14]. In fact, AID can deaminate deoxycytidine of DNA *in vitro*[15–17]. This hypothesis was also supported by the finding that the base specificity of SHM is perturbed and the efficiency of CSR is reduced with inhibition or deficiency of uracil DNA glycosylase[18,19].

Although AID is involved in both CSR and SHM, these two reactions have distinctly different products and probably require mechanisms that are different, at least in part. In addition, CSR and SHM are independent events, as some IgM molecules accumulate SHM and some IgG molecules have no mutations. Spleen cells stimulated by lipopolysaccharide (LPS) *in vitro* usually undergo CSR but not SHM. It would therefore be useful to understand how B lymphocytes differentially regulate CSR and SHM. How can a single protein, AID, differentially regulate V-region point mutation and S-region recombination in activated B cells? The distinction is likely to occur at two stages: recognition of target and mode of enzymatic reaction. Although the targets of CSR and SHM have no primary sequence specificity[20–24], there are some indications that higher-order DNA structures might be recognized by enzymes involved in these reactions[23–29]. Enzymatic reactions that cleave V and S regions may require different cofactors and thus may mediate different types of cleavage. SHM reactions in the V region probably require either single-strand or no cleavage[18,30], whereas CSR reactions depend on cleavage of both DNA strands[31,32].

Studies of mutations in the gene encoding AID (official gene name,

[1]Inserm U429, Hopital Necker-Enfants Malades, 149 Rue de Sevres, Paris, France. [2]Department of Pediatrics, National Defense Medical College, 3-2 Namiki, Tokorozawa, Saitama, 359-8513, Japan. [3]Department of Pediatrics and Developmental Biology, Graduate School of Medicine, Tokyo Medical and Dental University, 1-5-45 Yushima, Bunkyo-ku, Tokyo, 113-8519, Japan. [4]Department of Medical Chemistry, Graduate School of Medicine, Kyoto University, Yoshida, Sakyo-ku, Kyoto, 606-8501, Japan. Correspondence should be addressed to T.H. (honjo@mfour.med.kyoto-u.ac.jp).

Published online 10 August 2003; doi:10.1038/ni964

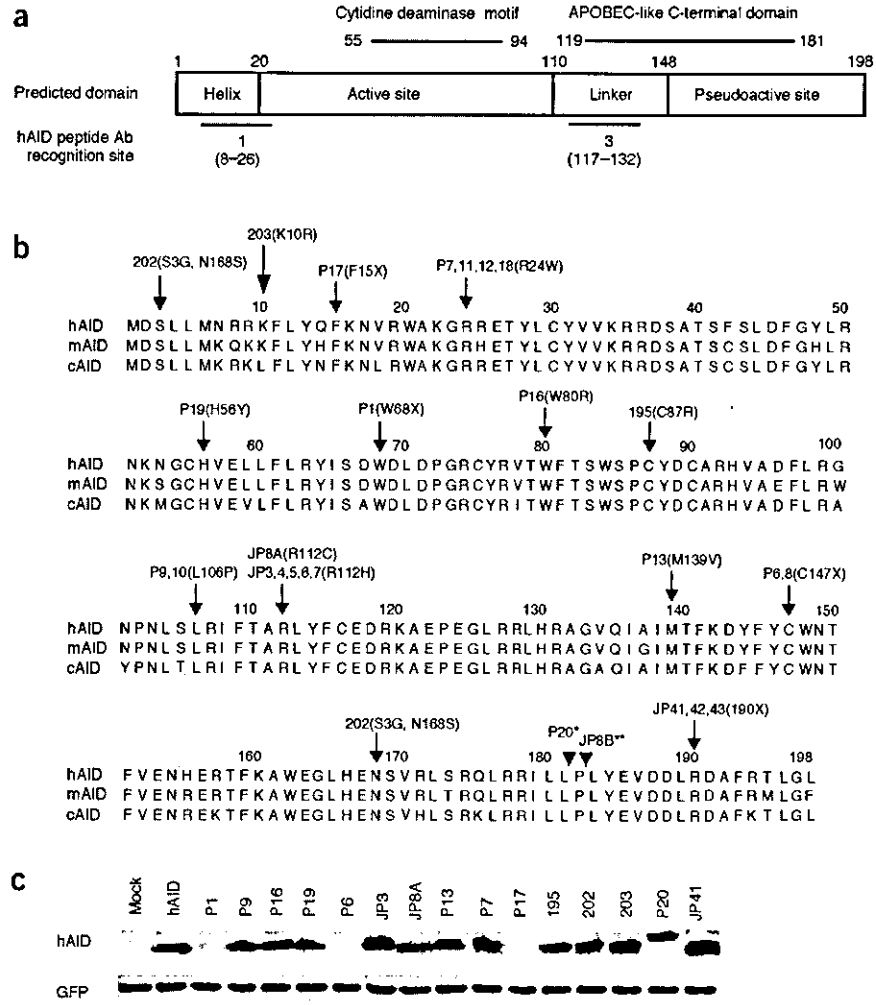

Figure 1 Mapping of AID mutants and sequence conservation of AID. (**a**) Proposed domain structure of APOBEC-1 (ref. 35), adopted to AID. The APOBEC-like C-terminal domain was retrieved from the conserved domain database with reverse-position-specific BLAST. Bottom, amino acid regions used for generation of peptide antibodies (Ab #1 and Ab #3). hAID, human AID. (**b**) Locations of AID mutants and conservation of AID sequences. Locations of replacements and insertions of amino acids in AID mutants are indicated by arrows and arrowheads, respectively. Amino acid replacement and position of each mutant are in parentheses. X, mutations causing truncations. Shaded amino acids indicate those conserved among human (h), and mouse (m) and chicken (c). *, insertion of 34 residues (VTKPSTQFRRLSGPTDPQPRFEAIHSICFSLSLR); **, frameshift replacement of the C terminus with 26 residues (CMRLMTYETHFVLWDFDSNFQEC HTR). (**c**) Expression of AID mutant proteins. 293T cells were transiently transfected with plasmids expressing AID mutants (above blots). After 3 d, cell extracts were prepared for immunoblot analysis, and human AID (hAID) was detected using anti-AID (Ab #1). Bottom, GFP coexpression determined using anti-GFP (internal control). Data are representative of three experiments. Mock, vector alone.

AICDA) in patients with hyper-IgM syndrome type 2 (HIGM2) have shown that loss-of-function point mutations are scattered throughout the entire coding region of this gene[6,33,34]. In addition, almost all 198 amino acid residues of AID are strongly conserved among chicken, mouse and human[4,9,11]. These results indicate two possibilities: that AID requires a cofactor(s) that interacts with various domains, and that conformational constraints on AID structure are very rigorous. Here, we report that mutations in the C-terminal domain of human AID resulted in loss of CSR function, but that the AID mutants retained SHM and *E. coli* mutagenesis activity. These results indicate that AID activity depends on interaction with CSR-specific cofactors at its C-terminal region.

RESULTS

Characterization of AID mutants

We studied AID mutants in patients with HIGM2 previously published[6,33,34] and newly identified in Europe and Japan, and artificial mutants (195, 202 and 203) generated by PCR of human AID cDNA (Fig. 1). Sixteen mutations were dispersed in four functional domains of AID originally proposed for APOBEC-1 by comparison with the three-dimensional structure of *E. coli* metabolic cytidine deaminase[35]. Among these, four (P1, P16, P19 and 195) were mapped in the cytidine deaminase motif, a putative catalytic center of AID; two (P7 and P9) were mapped in the active site but outside the cytidine deaminase motif; two (203 and P17) were mapped in the N-terminal α-helix region; four (JP3, JP8A, P6 and P13) were mapped in the linker region; three (P20, JP41 and JP8B) were mapped in the C-terminal pseudoactive site that has the structural homology with the active site; and one (202) had double mutations in the α-helix and pseudoactive site. Among the mutations analyzed, three mutant proteins (P1, P6 and P17) were not detectable, probably because of truncation mutations (Fig. 1c). Cells with the other mutations produced amounts of mutant AID similar to that of wild-type AID. Although those patients with homozygous mutations[6,33,34] showed almost complete loss of function of CSR activity, some had low concentrations of serum IgG (P16) or marginal mutations in the V_H3-23 gene (P8 and P18; Table 1). As immunoglobulin transfusion, clonal reversion mutation, selection and PCR artifacts may perturb the phenotypes of AID mutations in the patients with HIGM2, we examined the activity of each mutant AID *in vitro*.

Mutations specific to CSR

To understand the molecular mechanisms of these mutations, we did *in vitro* assays that allowed us to measure the activity of CSR and SHM of each mutant in a quantitative manner[7,8]. We used spleen B cells from AID-deficient mice to monitor the CSR activity of each mutant. We inserted mutated cDNA encoding AID flanked by internal ribosome entry site (IRES) and green fluorescence protein (GFP) sequences into a retroviral vector and used this to infect stimulated AID-deficient spleen B cells[36]. Then, 3 d later, we quantified surface